Inorg. Chem. **2009**, *48*, 1449−1468

Synthesis, Crystal Structures, and Photoluminescent Properties of the Cu(I)/X/α,ω-Bis(benzotriazole)alkane Hybrid Family (X = Cl, Br, I, and CN)

Man-Cheng Hu,*,† Yan Wang,† Quan-Guo Zhai,*,† Shu-Ni Li,† Yu-Cheng Jiang,† and Yong Zhang‡

Key Laboratory of Macromolecular Science of Shaanxi Province, School of Chemistry and Materials Science, Shaanxi Normal University, Xi'an, 710062, Shaanxi, P. R. China, and School of Chemistry and Chemical Engineering, Suzhou University, Suzhou 215123, Jiangsu, P. R. China

Received August 19, 2008

This work focused on a systematic investigation of the influences of the spacer length of the flexible α,ω-bis(benzotriazole)alkane ligands and counteranions on the overall molecular architectures of hybrid structures that include Cu(I). Using the self-assembly of CuX (X = Cl, Br, I, or CN) with the five structurally related flexible organic ligands (**L1**−**L5**) under hydro(solvo)thermal conditions, we have synthesized and characterized 10 structurally unique materials of the Cu(I)/X/α,ω-bis(benzotriazole)alkane organic−inorganic hybrid family, $\{[CuCl]_2(\mathbf{L1})\}_n$ (**1**), $\{[CuBr](\mathbf{L2})\}_n$ (**2**), $\{[CuCl]_2(\mathbf{L3})\}_n$ (**3**), $\{[CuI]_2(\mathbf{L4})\}_n$ (**4**), $\{[CuBr]_2(\mathbf{L4})\}_n$ (**5**), $\{[CuBr]_3(\mathbf{L5})\}_n$ (**6**), $\{[CuCN]_2(\mathbf{L1})\}_n$ (**7**), $\{[CuCl]_4(\mathbf{L2})\}_n$ (**8**), $\{[CuBr]_4(\mathbf{L2})\}_n$ (**9**), and $\{[CuCl]_2(\mathbf{L4})\}_n$ (**10**), by means of elemental analyses, X-ray powder diffraction, Fourier transform infrared spectroscopy, thermogravimetric analysis, and photoluminescence measurements. Single-crystal X-ray analyses showed that the inorganic subunits in these compounds were $\{Cu_2X_2\}$ binuclear clusters (**1** and **2**), $\{Cu_4X_4\}$ cubane clusters (**4**, **5**, and **10**), $\{CuX\}_n$ single chains (**3** and **7**), a $\{Cu_3X_3\}_n$ ladderlike chain (**6**), and unprecedented $\{Cu_8X_8\}_n$ ribbons (**8** and **9**). The increasing dimensionality from 1-D (**1**−**4**) to 2-D (**5** and **6**) to 3-D (**7**−**10**) indicates that the spacer length and isomerism of the bis(benzotriazole)alkane ligands play an essential role in the formation of the framework of the Cu(I) hybrid materials. The influence of counteranions and $\pi-\pi$ stacking interactions on the formation and dimensionality of these hybrid coordination polymers has also been explored. In addition, all the complexes exhibit high thermal stability and strong fluorescence properties in the solid state at ambient temperature.

Introduction

The significant contemporary interest in organic−inorganic hybrid solid materials reflects both the fundamental chemistry of the rational design of complex materials and practical applications in fields such as ion-exchange,[1] optical materials,[2] multiphase catalysis,[3] and gas storage.[4] Such materials combine the unique features of the inorganic and organic components in a complementary fashion. The inorganic component may confer useful optical or magnetic properties and thermal stability, whereas the organic component offers the potential for a range of polarizabilities and structural diversification. The combination of the characteristics of the organic and inorganic components gives rise to diverse structural chemistry and novel physical properties and provides access to a vast domain of multifunctional materials.[5]

By varying the choice of inorganic components, researchers have expanded this domain from aluminosilicates to many other inorganic microstructures. Most of these components are based on oxygen-containing materials, especially metal oxides, but there are many examples based on other chemistries, such as nitrides, sulfides, and halides. Among the various families of inorganic components, the family of metal halides or pseudohalides is important.[6] With regard to the metal center, the Cu(I) cation is particularly well-suited

* To whom correspondence should be addressed. E-mail: hmch@snnu.edu.cn (M.-C.H.), zhaiqg@snnu.edu.cn (Q.-G.Z.). Phone: +86-29-85307765. Fax: +86-29-85307774.

† Shaanxi Normal University.

‡ Suzhou University.

(1) For examples, see: (a) Muthu, S.; Yip, J. H. K.; Vittal, J. J. *J. Chem. Soc., Dalton Trans.* **2002**, 4561. (b) Fan, J.; Gan, L.; Kawaguchi, H.; Sun, W. Y.; Yu, K. B.; Tang, X. *Chem.−Eur. J.* **2003**, *9*, 3965. (c) Lin, Z. Z.; Jiang, F. L.; Yuan, D. Q.; Chen, L.; Zhou, Y. F.; Hong, M. C. *Eur. J. Inorg. Chem.* **2005**, 1927. (d) Custelcean, R.; Haverlock, T. J.; Moyer, B. A. *Inorg. Chem.* **2006**, *45*, 6446.

10.1021/ic801574k CCC: $40.75
Published on Web 01/20/2009

for such studies; its coordination number may vary from two to five and the associated counteranion X (X = Cl, Br, I, CN, or SCN) can be incorporated as an essential element of the framework. Thus, various nuclearities and high structural complexities may be achieved.[6c] Moreover, the presence of direct Cu···Cu interactions has been shown to be one of the crucial causes of the luminescence properties of such species.[7] To our knowledge, the basic copper(I) halide or pseudohalide (CuX) skeletons generally exhibit several structural motifs:[8] rhomboid Cu_2X_2 dimers, cubane or step-cubane Cu_4X_4 tetramers, zigzag $[CuX]_n$ chains, double-stranded $[Cu_2X_2]_n$ ladders, and hexagonal $[Cu_6X_6]_n$ grid chains. Usually, rigid or flexible multidentate nitrogen-donor ligands act as organic connectors to link these CuX motifs to form extended organic−inorganic hybrid architectures varying from one to three dimensions.[6,7,8g,9] On the other hand, several examples show that the dimensionality of such hybrid materials can be influenced predominantly by the coordination properties of the organic ligands. Although a large number of organic molecules have been investigated to date, polypyridine ligands have witnessed the most important development. However, other ligands can provide different tether lengths, charge-balance requirements, and functional group orientations. More recently, polyazaheteroaromatic compounds such as pyrazole, imidazole, triazole, and tetrazole in their neutral and anionic forms have been successfully exploited in the construction of complex organic−inorganic hybrid architectures.[10] In addition to providing structural diversity and unusual magnetochemistry, the azolates allow the design of materials with interactions between closed-shell d^{10} metal cations, providing a route to new luminescent materials. A number of binary Cu(I)/pyrazolates and Cu(I)/triazolates with photoluminescent properties have been described;[10h,11] however, hybrid solids constructed from polyazaheteroaromatic compounds and Cu(I) halides or pseudohalides are rare, especially for high dimensional networks.[8]

As an extension of our previous study of the family of Cu(I)/Ag(I)/1,2,4-triazole/polyoxometalate hybrids,[12] we have embarked on a program in which hydro(solvo)thermal syntheses are used to discover new hybrid solids based on inorganic CuX (X = Cl, Br, I, CN, or SCN) subunits and α,ω-bis(benzotriazole)alkane organic ligands. Compared to flexible ligands incorporating other heterocycles such as imidazole,[13] benzoimidazole,[14] and triazole,[15] the flexible benzotriazole ligands have been investigated less often and in less depth.[16] To the best of our knowledge, no investigation has been carried out on the hydrothermal or solvothermal synthesis of hybrid materials constructed from flexible benzotriazole ligands. To probe the influence of systematic variations in ligand structure and in counteranions on the overall hybrid architecture, we prepared a series of α,ω-bis(benzotriazole)alkane ligands: 1,2-bis(benzotriazol-1-yl)ethane (**L1**), 1,2-bis(benzotriazol-1,2-yl)ethane (**L2**), 1,3-bis(benzotriazol-1-yl)propane (**L3**), 1,4-bis(benzotriazol-1-yl)butane (**L4**), and 1,3-bis(benzotriazol-2-yl)propane (**L5**) (Scheme 1). In the present study, we synthesized and characterized 10 Cu(I) hybrid solids of these ligands: $\{[CuCl]_2(\mathbf{L1})\}_n$ (**1**), $\{[CuBr](\mathbf{L2})\}_n$ (**2**), $\{[CuCl]_2(\mathbf{L3})\}_n$ (**3**), $\{[CuI]_2(\mathbf{L4})\}_n$ (**4**), $\{[CuBr]_2(\mathbf{L4})\}_n$ (**5**), $\{[CuBr]_3(\mathbf{L5})\}_n$ (**6**), $\{[CuCN]_2(\mathbf{L1})\}_n$ (**7**), $\{[CuCl]_4(\mathbf{L2})\}_n$ (**8**), $\{[CuBr]_4(\mathbf{L2})\}_n$ (**9**), and $\{[CuCl]_2(\mathbf{L4})\}_n$ (**10**). This series of complexes (**1**−**10**)

(2) (a) Evans, O. R.; Lin, W. B. *Chem. Mater.* **2001**, *13*, 3009. (b) Sanchez, C.; Lebeau, B.; Chaput, F.; Boilet, J. P. *Adv. Mater.* **2003**, *15*, 1969. (c) Zheng, X. J.; Sun, C. Y.; Lu, S. Z.; Liao, F. H.; Gao, S.; Jin, L. *Eur. J. Inorg. Chem.* **2004**, 3262. (d) He, J. H.; Yu, J. H.; Zhang, Y. T.; Pan, Q. H.; Xu, R. R. *Inorg. Chem.* **2005**, *44*, 9279. (e) Yang, J.; Yuo, Q.; Li, G. D.; Cao, J. J.; Li, G. H.; Chen, J. S. *Inorg. Chem.* **2006**, *45*, 2857.

(3) (a) Fujita, M.; Kwon, Y. J.; Washizu, S.; Ogura, K. *J. Am. Chem. Soc.* **1994**, *116*, 1151. (b) Seo, J. S.; Whang, D.; Lee, H.; Jun, S. I.; Oh, J.; Jeon, Y. J.; Kim, K. *Nature* **2000**, *404*, 982. (c) Evans, O. R.; Ngo, H. L.; Lin, W. B. *J. Am. Chem. Soc.* **2001**, *123*, 10395. (d) Ngo, H. L.; Hu, A. G.; Lin, W. B. *J. Mol. Catal. A* **2004**, *215*, 177. (e) Wu, C. D.; Hu, A.; Zhang, L.; Lin, W. B. *J. Am. Chem. Soc.* **2005**, *127*, 8940.

(4) (a) Kitaura, R.; Kitagawa, S.; Kubtoa, Y.; Kobayashi, T. C.; Kindo, K.; Mita, Y.; Matsuo, A.; Kobayashi, M.; Chang, H. C.; Ozawa, T. C.; Suzuki, M.; Sakata, M.; Takata, M. *Science* **2002**, *298*, 2358. (b) Rosi, N. L.; Eckert, J.; Eddaoudi, M.; Vodak, D. T.; Kim, J.; O'Keeffe, M.; Yaghi, O. M. *Science* **2003**, *300*, 1127. (c) Rowsell, J. L. C.; Millward, A. R.; Park, K. S.; Yaghi, O. M. *J. Am. Chem. Soc.* **2004**, *126*, 5666. (d) Chen, B. L.; Ockwig, N. W.; Millward, A. R.; Contreras, D. S.; Yaghi, O. M. *Angew. Chem., Int. Ed.* **2005**, *44*, 4745. (e) Chun, H.; Dybtsev, D. N.; Kim, H.; Kim, K. *Chem.—Eur. J.* **2005**, *11*, 3521. (f) Rowsell, J. L. C.; Yaghi, O. M. *J. Am. Chem. Soc.* **2006**, *128*, 1304.

(5) (a) Ouellette, W.; Hudson, B. S.; Zubieta, J. *Inorg. Chem.* **2007**, *46*, 4887, and references therein. (b) Ouellette, W.; Prosvirin, A. V.; Valeich, J.; Dunbar, K. R.; Zubieta, J. *Inorg. Chem.* **2007**, *46*, 9067.

(6) (a) Li, D.; Shi, W. J.; Hou, L. *Inorg. Chem.* **2005**, *44*, 3907. (b) Cariati, E.; Roberto, D.; Ugo, R.; Ford, P. C.; Galli, S.; Sironi, A. *Inorg. Chem.* **2005**, *44*, 4077. (c) Peng, R.; Li, D.; Wu, T.; Zhou, X. P.; Ng, S. W. *Inorg. Chem.* **2006**, *45*, 4035.

(7) Ford, P. C.; Cariati, E.; Bourassa, J. *Chem. Rev.* **1999**, *99*, 3625.

(8) (a) Graham, P. M.; Pike, R. D.; Sabat, M.; Bailey, R. D.; Pennington, W. T. *Inorg. Chem.* **2000**, *39*, 5121, and references therein. (b) Healy, P. C.; Pakawatchai, C.; Raston, C. L.; Skelton, B. W.; White, A. H. *J. Chem. Soc., Dalton Trans.* **1983**, 1905. (c) Healy, P. C.; Pakawatchai, C.; White, A. H. *J. Chem. Soc., Dalton Trans.* **1983**, 1917. (d) Barron, P. F.; Dyason, J. C.; Engelhardt, L. M.; Healy, P. C.; White, A. H. *Inorg. Chem.* **1984**, *23*, 3766. (e) Alyea, E. C.; Ferguson, G.; Malito, J.; Ruhl, B. L. *Inorg. Chem.* **1985**, *24*, 3720. (f) Lu, J.; Crisci, G.; Niu, T.; Jacobson, A. J. *Inorg. Chem.* **1997**, *36*, 5140. (g) Li, G.; Shi, Z.; Liu, X.; Dai, Z.; Feng, S. *Inorg. Chem.* **2004**, *43*, 6884.

(9) (a) Geiser, U.; Willett, R. D.; Lindbeck, M.; Ertherson, K. *J. Am. Chem. Soc.* **1986**, *108*, 1173. (b) Lu, J. Y.; Cabrera, B. R.; Wang, R. J.; Li, J. *Inorg. Chem.* **1998**, *37*, 4480. (c) Lu, J. Y.; Cabrera, B. R.; Wang, R.-J.; Li, J. *Inorg. Chem.* **1999**, *38*, 4608. (d) Chesnut, D. J.; Kusnetzow, A.; Birge, R. R.; Zubieta, J. *Inorg. Chem.* **1999**, *38*, 2663. (e) Blake, A. J.; Brooks, N. R.; Champness, N. R.; Cooke, P. A.; Deveson, A. M.; Fenske, D.; Hubberstey, P.; Li, W. S.; Schröder, M. *J. Chem. Soc., Dalton Trans.* **1999**, 2103, and references therein. (f) Willett, R. D. *Inorg. Chem.* **2001**, *40*, 966. (g) Hu, S.; Tong, M. L. *Dalton Trans.* **2005**, 1165.

(10) (a) Potts, K. T. *Chem. Rev.* **1961**, *61*, 87. (b) Haasnoot, J. G. *Coord. Chem. Rev.* **2000**, *200*, 131. (c) Ferrer, S.; Lloret, F.; Bertomeu, I.; Alzuet, G.; Borras, J.; Garcia-Granda, S.; Liu-Gonzalez, M.; Haasnoot, J. G. *Inorg. Chem.* **2002**, *41*, 5821. (d) Beckmann, U.; Brooker, S. *Coord. Chem. Rev.* **2003**, *245*, 17. (e) Klingele, M. H.; Brooker, S. *Coord. Chem. Rev.* **2003**, *241*, 119. (f) Zhang, J. P.; Zhang, S. L.; Huang, X. C.; Chen, X. M. *Angew. Chem., Int. Ed.* **2004**, *43*, 206. (g) Yi, L.; Ding, B.; Zhao, B.; Cheng, P.; Liao, D. Z.; Yan, S. P.; Jiang, Z. H. *Inorg. Chem.* **2004**, *43*, 33. (h) Zhang, J. P.; Lin, Y. Y.; Huang, X. C.; Chen, X. M. *J. Am. Chem. Soc.* **2005**, *127*, 5495. (i) Zhang, J. P.; Lin, Y. Y.; Zhang, W. X.; Chen, X. M. *J. Am. Chem. Soc.* **2005**, *127*, 14162. (j) Zhou, J. H.; Cheng, R. M.; Song, Y.; Li, Y. Z.; Yu, Z.; Chen, X. T.; Xue, Z. L.; You, X. Z. *Inorg. Chem.* **2005**, *44*, 8011. (k) Zhang, J. P.; Chen, X. M. *Chem. Commun.* **2006**, 1689.

(11) (a) Dias, H. V. R.; Diyabalange, H. V. K.; Eldabaja, M. G.; Elbjeirami, O.; Rawashdeh-Omary, M. A.; Omary, M. A. *J. Am. Chem. Soc.* **2005**, *127*, 7489. (b) Omary, M. A.; Rawashdeh-Omary, M. A.; Gonser, M. W. A.; Elbjeirami, O.; Grimes, T.; Cundair, T. R. *Inorg. Chem.* **2005**, *44*, 8200.

(12) Zhai, Q. G.; Wu, X. Y.; Chen, S. M.; Zhao, Z. G.; Lu, C. Z. *Inorg. Chem.* **2007**, *46*, 5046.

Scheme 1

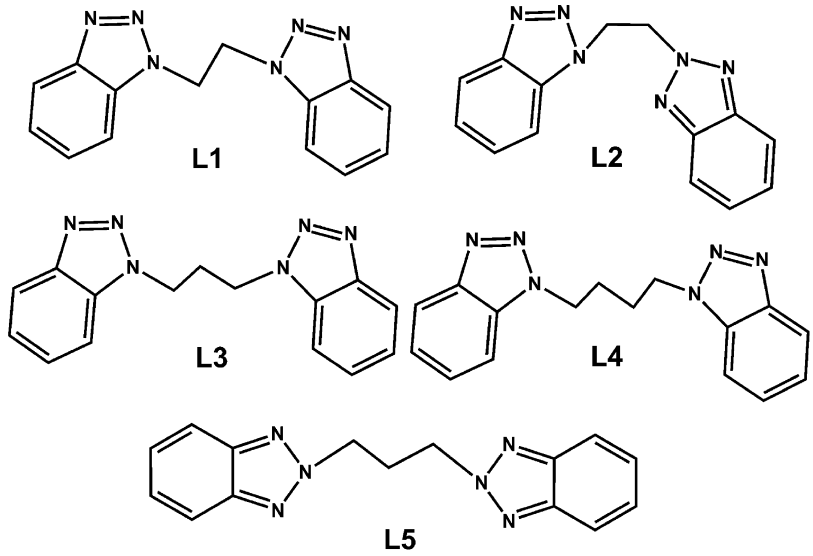

showed an increasing dimensionality from 1-D to 3-D, thereby providing an opportunity to systematically probe the effects of modifying the length of the alkane and alternating the counteranions on the precise topography of the compounds in this hybrid family. Moreover, these hybrid complexes may be excellent candidates for photoactive materials because they all exhibit high thermal stability and strong fluorescent properties.

Experimental Section

Materials and Methods. The ligands **L1**−**L5** were prepared according to the methods previously described in the research literature.[16c,17] Other reagents and solvents were commercially available and used without further purification. C, H, and N elemental analyses were performed using an Elementar Vario EL III elemental analyzer. The FT-IR spectra (KBr pellets) were recorded using a Nicolet Avatar 360 FT-IR spectrometer in the range of 4000−400 cm^{-1}. The fluorescence spectra were measured with a Cary Eclipse fluorescence spectrophotometer at room temperature using powdered crystal samples. The excitation slit and emission slit were both set at 2.5 nm. Thermal stability studies were carried out using a NETSCHZ STA-449C thermoanalyzer under a nitrogen atmosphere (40−1000 °C range) at a heating rate of 10 °C/min.

Preparations. A. $\{[CuCl]_2(L1)\}_n$ (1). A mixture of $CuCl_2 \cdot 2H_2O$ (0.172 g, 1.0 mmol), **L1** (0.132 g, 0.5 mmol), and water (10 mL) was stirred for 20 min in air and then heated at 180 °C for 72 h in a 25 mL, Teflon-lined reactor under autogenous pressure. Light-yellow, block-shaped crystals of **1** were obtained after the reaction solution cooled gradually (5 °C h^{-1}). These were then washed with water and air-dried. Yield: 0.042 g (ca. 18% based on the Cu). Anal. Calcd (%) for $C_{14}H_{12}N_6Cu_2Cl_2$: C, 36.34; H, 2.60; N, 18.17. Found (%): C, 36.36; H, 2.57; N, 18.18. IR (solid KBr pellet/cm^{-1}): 3436 (m), 3083 (w), 3030 (w), 2980 (w), 2932 (w), 2429 (w), 2358 (w), 1775 (w), 1614 (w), 1495 (w), 1416 (m), 1381 (s), 1358 (s), 1188 (m), 1040 (w), 818 (m), 753(s).

B. $\{[CuBr](L2)\}_n$ (2). A mixture of CuBr (0.144 g, 1.0 mmol), **L2** (0.264 g, 1.0 mmol), KBr (0.06 g, 0.5 mmol), and water (10.0 mL) was stirred for 30 min in air and then heated at 160 °C for 72 h in a 25 mL, Teflon-lined reactor under autogenous pressure. Garnet, prism-shaped crystals of **2** were obtained after the reaction solution cooled gradually (5 °C h^{-1}). These were then washed with water and air-dried. Yield: 0.285 g (ca. 70% based on the Cu). Anal. Calcd (%) for $C_{14}H_{12}N_6CuBr$: C, 41.2; H, 2.94; N, 20.6. Found (%): C, 41.08; H, 2.79; N, 21.1. IR (solid KBr pellet/cm^{-1}): 3430 (m), 3084 (w), 2976 (w), 2932 (w), 1602 (m), 1524 (w), 1494 (m), 1441 (m), 1318 (m), 1182 (m), 1036 (w), 754 (s).

C. $\{[CuCl]_2(L3)\}_n$ (3). A mixture of $CuCl_2 \cdot 2H_2O$ (0.172 g, 1.0 mmol), **L3** (0.139 g, 0.5 mmol), and water (10 mL) was stirred for 20 min in air and then heated at 180 °C for 72 h in a 25 mL, Teflon-lined reactor under autogenous pressure. Light-yellow, block-shaped crystals of **3** were obtained after the reaction solution cooled gradually (5 °C h^{-1}). These were then washed with water and air-dried. Yield: 0.031 g (ca. 13% based on the Cu). Anal. Calcd (%) for $C_{15}H_{14}N_6Cu_2Cl_2$: C, 37.79; H, 2.94; N, 17.64. Found (%): C, 37.69; H, 2.90; N, 17.66. IR (solid KBr pellet/cm^{-1}): 3436 (m),

(13) (a) Duncan, P. C. M.; Goodgame, D. M. L.; Menzer, S.; Williams, D. J. *Chem. Commun.* **1996**, 2127. (b) Hoskin, B. F.; Robson, R.; Slizys, D. A. *Angew. Chem., Int. Ed. Engl.* **1997**, *36*, 2336. (c) Hoskin, B. F.; Robson, R.; Slizys, D. A. *J. Am. Chem. Soc.* **1997**, *119*, 2952. (d) Ma, J. F.; Liu, J. F.; Xing, Y.; Jia, H. Q.; Lin, Y. H. *J. Chem. Soc., Dalton Trans.* **2000**, 2403. (e) Fan, J.; Sun, W. Y.; Okamura, T. A.; Zheng, Y. Q.; Sui, B.; Tang, W. X.; Ueyama, N. *Cryst. Growth Des.* **2004**, *4*, 579.

(14) (a) Tan, H. Y.; Zhang, H. X.; Ou, H. D.; Kang, B. S. *Inorg. Chim. Acta.* **2004**, *357*, 869. (b) Gilbert, J. G.; Addison, A. W.; Prabakaran, P.; Butcher, R. J.; Bocelli, G. *Inorg. Chem. Commun.* **2004**, *7*, 701.

(15) (a) Li, B. L.; Xu, Z.; Cao, Z. B.; Zhu, L. M.; Yu, K. B. *Transition Met. Chem.* **1999**, *24*, 622. (b) Tang, L. F.; Wang, Z. H.; Chai, J. F.; Jia, W. L.; Xu, Y. M.; Wang, J. T. *Polyhedron* **2000**, *19*, 1049. (c) Albada, G. A.; Guijt, R. C.; Haasnoot, J. G.; Lutz, M.; Spek, A. L.; Reedijk, J. *Eur. J. Inorg. Chem.* **2000**, 121. (d) Zhao, Q. H.; Li, H. F.; Wang, X. F.; Chen, Z. D. *New J. Chem.* **2002**, *26*, 1709. (e) Li, B.; Zhu, X.; Zhou, J.; Peng, Y.; Zhang, Y. *Polyhedron* **2004**, *23*, 3133. (f) Zhou, J.; Zhu, X.; Zhang, Y.; Li, B. *Inorg. Chem. Commun.* **2004**, *7*, 949. (g) Li, B.; Peng, Y.; Li, B.; Zhang, Y. *Chem. Commun.* **2005**, 2333. (h) Peng, Y. F.; Ge, H. Y.; Li, B. Z.; Li, B. L.; Zhang, Y. *Cryst. Growth Des.* **2006**, *6*, 994.

(16) (a) Hou, H. W.; Meng, X. R.; Song, Y. L.; Fan, Y. T.; Zhu, Y.; Lu, H. J.; Du, C. X.; Shao, W. T. *Inorg. Chem.* **2002**, *41*, 4068. (b) Meng, X. R.; Song, Y. L.; Hou, H. W.; Fan, Y. T.; Li, G.; Zhu, Y. *Inorg. Chem.* **2003**, *42*, 1306. (c) Borsting, P.; Steel, P. J. *Eur. J. Inorg. Chem.* **2004**, 376. (d) Zhou, J.; Peng, Y.; Zhang, Y. P.; Li, B.; Zhang, Y. *Inorg. Chem. Commun.* **2004**, *7*, 1181. (e) Zhou, J.; Liu, X.; Zhang, Y. P.; Li, B.; Zhang, Y. *Inorg. Chem. Commun.* **2006**, *9*, 216. (f) Jones, L. F.; Dea, L. O.; Offermann, D. A.; Jensen, P.; Moubaraki, B.; Murray, K. S. *Polyhedron* **2006**, *25*, 360.

(17) Xie, X. J.; Yang, G. S.; Cheng, L.; Wang, F. *Huaxue Shiji* **2000**, *22*, 222.

3073 (w), 3001 (w), 2921 (w), 2851 (w), 1778 (w), 1615 (w), 1495 (w), 1451 (m), 1417 (m), 1380 (s), 1358 (s), 1193 (m), 809 (m), 748 (m).

D. {[CuI]$_2$(L4)}$_n$ (4). A mixture of CuI (0.192 g, 1.0 mmol), **L4** (0.146 g, 0.5 mmol), KI (0.083 g, 0.5 mmol), and water (10.0 mL) was stirred for 30 min in air and then heated at 180 °C for 120 h in a 25 mL, Teflon-lined reactor under autogenous pressure. Light-yellow, block-shaped crystals of **4** were obtained after the reaction solution cooled gradually (5 °C h $^{-1}$). These were then washed with water and air-dried. Yield: 0.10 g (ca. 30% based on the Cu). Anal. Calcd (%) for $C_{16}H_{16}N_6Cu_2I_2$: C, 28.5; H, 2.38; N, 12.48. Found (%): C, 28.48; H, 2.35; N, 12.58. IR (solid KBr pellet/cm^{-1}): 3430 (m), 3053 (w), 2920 (m), 2853 (w), 1596 (m), 1488 (w), 1448 (m), 1311 (s), 1229 (m), 1172 (m), 992 (m), 783 (m), 735 (s).

E. {[CuBr]$_2$(L4)}$_n$ (5). A mixture of CuBr (0.144 g, 1.0 mmol), **L4** (0.146 g, 0.5 mmol), KBr (0.12 g, 1.0 mmol), and acetonitrile (6.0 mL) was stirred for 30 min in air and then heated at 170 °C for 120 h in a 25 mL, Teflon-lined reactor under autogenous pressure. Garnet, block-shaped crystals of **5** were obtained after the reaction solution cooled gradually (5 °C h $^{-1}$). These were then washed with acetonitrile and air-dried. Yield: 0.115 g (ca. 40% based on the Cu). Anal. Calcd (%) for $C_{16}H_{16}N_6Cu_2Br_2$: C, 33.15; H, 2.76; N, 14.50. Found (%): C, 33.12; H, 2.74; N, 14.60. IR (solid KBr pellet/cm^{-1}): 3431 (m), 3055 (w), 2941 (w), 1600 (m), 1486 (m), 1446 (m), 1302 (m), 1225 (m), 1171 (s), 1051 (m), 986 (m), 746 (s).

F. {[CuBr]$_3$(L5)}$_n$ (6). A mixture of CuBr (0.216 g, 1.5 mmol), **L5** (0.139 g, 0.5 mmol), KBr (0.12 g, 1.0 mmol), and water (10.0 mL) was stirred for 30 min in air and then heated at 170 °C for 120 h in a 25 mL, Teflon-lined reactor under autogenous pressure. Yellow, block-shaped crystals of **6** were obtained after the reaction solution cooled gradually (5 °C h $^{-1}$). These were then washed with water and air-dried. Yield: 0.23 g (ca. 65% based on the Cu). Anal. Calcd (%) for $C_{15}H_{14}N_6Cu_3Br_3$: C, 25.40; H, 1.98; N, 11.85. Found (%): C, 25.32; H, 1.78; N, 11.95. IR (solid KBr pellet/cm^{-1}): 3425 (m), 3055 (w), 2953 (w), 2923 (w), 1631 (m), 1560 (m), 1434 (m), 1386 (m), 1314 (m), 1273 (m), 1195 (m), 848 (m), 740 (s).

G. {[CuCN]$_2$(L1)}$_n$ (7). A mixture of CuCN (0.18 g, 2.0 mmol), **L1** (0.264 g, 1.0 mmol), $K_3Fe(CN)_6 \cdot 3H_2O$ (0.165 g, 0.5 mmol), and water (10.0 mL) was stirred for 20 min in air and then heated at 180 °C for 72 h in a 25 mL, Teflon-lined reactor under autogenous pressure. Yellow, block-shaped crystals of **7** were obtained after the reaction solution cooled gradually (5 °C h $^{-1}$). These were then washed with water and air-dried. Yield: 0.129 g (ca. 29% based on the Cu). Anal. Calcd (%) for $C_{16}H_{12}N_8Cu_2$: C, 43.34; H, 2.73; N, 25.27. Found (%): C, 43.86; H, 2.51; N, 25.18. IR (solid KBr pellet/cm^{-1}): 3435 (s), 3085 (w), 2915 (w), 2103 (s), 1643 (m), 1452 (m), 1445 (s), 1311 (m), 1238 (m), 1080 (m), 872 (w), 739 (s).

H. {[CuCl]$_4$(L2)}$_n$ (8). A mixture of CuCl (0.20 g, 2.0 mmol), **L2** (0.132 g, 0.5 mmol), KCl (0.15 g, 2.0 mmol), and water (10.0 mL) was stirred for 30 min in air and then heated at 160 °C for 72 h in a 25 mL, Teflon-lined reactor under autogenous pressure. Orange, block-shaped crystals of **8** were obtained after the reaction solution cooled gradually (5 °C h $^{-1}$). These were then washed with water and air-dried. Yield: 0.064 g (ca. 20% based on the Cu). Anal. Calcd (%) for $C_{14}H_{12}N_6Cu_4Cl_4$: C, 25.44; H, 1.82; N, 12.72. Found (%): C, 25.41; H, 1.80; N, 12.74. IR (solid KBr pellet/cm^{-1}): 3492 (m), 3059 (w), 2973 (m), 1616 (w), 1559 (m), 1496 (w), 1444 (m), 1375 (w), 1328 (m), 1282 (m), 1207 (m), 1127 (m), 1046 (m), 873 (w), 746 (s).

I. {[CuBr]$_4$(L2)}$_n$ (9). The preparation of **9** was similar to that of **2**, except for the reaction temperature (160 °C for **2** and 180 °C for **9**). Garnet, block-shaped crystals of **9** were obtained after the reaction solution cooled gradually (5 °C h $^{-1}$). These were then washed with water and air-dried. Yield: 0.146 g (ca. 70% based on the Cu). Anal. Calcd (%) for $C_{14}H_{12}N_6Cu_4Br_4$: C, 20.09; H, 1.43; N, 10.02. Found (%): C, 20.13; H, 1.33; N, 10.12. IR (solid KBr pellet/cm^{-1}): 3455 (m), 3049 (w), 2974 (w), 1607 (w), 1562 (m), 1444 (m), 1327 (w), 1299 (m), 1204 (m), 1131 (m), 982 (m), 871 (m), 754 (s).

J. {[CuCl]$_2$(L4)}$_n$ (10). A mixture of $CuCl_2 \cdot 2H_2O$ (0.086 g, 0.5 mmol), **L4** (0.073 g, 0.25 mmol), and ethanol (8.0 mL) was stirred for 20 min in air and then heated at 160 °C for 72 h in a 25 mL, Teflon-lined reactor under autogenous pressure. Light-yellow, block-shaped crystals of **10** were obtained after the reaction solution cooled gradually (5 °C h $^{-1}$). These were then washed with ethanol and air-dried. Yield: 0.062 g (ca. 50% based on the Cu). Anal. Calcd (%) for $C_{16}H_{16}N_6Cu_2Cl_2$: C, 39.16; H, 3.26; N, 17.13. Found (%): C, 39.14; H, 3.22; N, 17.17. IR (solid KBr pellet/cm^{-1}): 3449 (m), 3059 (w), 2947 (m), 1616 (w), 1590 (m), 1489 (w), 1452 (m), 1326 (m), 1219 (m), 1162 (m), 1063 (m), 998 (w), 776 (m), 746 (s).

X-ray Crystallography. Suitable single crystals of **1**−**10** were carefully selected under an optical microscope and glued to thin glass fibers. Crystallographic data for all compounds were collected with a Siemens Smart CCD diffractometer with graphite-monochromated Mo Kα radiation (λ = 0.71073 Å) at T = 293(2) K. Absorption corrections were made using the SADABS program.[18] The structures were solved using the direct method and refined by full-matrix least-squares methods on F^2 by using the SHELXL-97 program package.[19] All non-hydrogen atoms were refined anistropically. Positions of the hydrogen atoms attached to carbon and nitrogen atoms were fixed at their ideal positions. Crystal data, as well as details of data collection and refinement for **1**−**10**, are summarized in Table 1. Selected bonded lengths and angles are listed in Tables 2 and 3. The structural characteristics are summarized in Table 4. CCDC-(698212−698221) (**1**−**10**) contain the supplementary crystallographic data for this paper. These data can be obtained free of charge from the Cambridge Crystallographic Data Centre at www.ccdc.cam.ac.uk/data_request/cif.

Results and Discussion

Syntheses. The flexible bis(benzotriazole)alkane ligands **L1**−**L5** were prepared by reaction of benzotriazole with 1,2-dibromoethane, 1,3-dibromopropane, and 1,4-dibromobutane using previously described methods.[16c,17] The reaction usually produces a mixture of the symmetrical 1,1′- and 2,2′-isomers, along with the asymmetrical 1,2′-isomer. These three isomers were separated by means of column chromatography on silica gel and recrystallized from absolute ethanol, as reported by Borsting and Steel.[16c] Crystals of **1**−**10** were synthesized directly with the corresponding metal/ligand ratios under hydro(solvo)thermal conditions, which produce a richer content of the desired compounds than is obtained using the conventional method. This is the first time that the hydrothermal or solvothermal method has been used to synthesize organic−inorganic hybrid materials based on flexible α,ω-bis(benzotriazole)alkane ligands. It is well-known that this method can produce metastable com-

(18) Sheldrick, G. M. *SADABS, Program for Area Detector Adsorption Correction*; University of Göttingen: Göttingen, Germany, 1996.
(19) Sheldrick, G. M. *SHELXL-97, Program for Solution of Crystal Structures*; University of Göttingen: Göttingen, Germany, 1997.

Table 1. Summary of the Crystal Data and Structure Refinement Parameters for **1**−**10**

	1	**2**	**3**	**4**	**5**
empirical formula	$C_{14}H_{12}N_6Cu_2Cl_2$	$C_{14}H_{12}N_6CuBr$	$C_{15}H_{14}N_6Cu_2Cl_2$	$C_{16}H_{16}N_6Cu_2I_2$	$C_{16}H_{16}N_6Cu_2Br_2$
fw	462.28	407.75	476.30	673.23	579.25
cryst syst	monoclinic	monoclinic	triclinic	tetragonal	tetragonal
space group	*C*2/*c*	*C*2/*c*	$P\bar{1}$	*P*4(1)22	*P*4(2)/*n*
a (Å)	7.5098(15)	18.001(2)	4.0289(8)	11.9208(16)	13.4900(14)
b (Å)	15.068(3)	10.1463(15)	14.208(3)	11.9208(16)	13.4900(14)
c (Å)	13.534(3)	16.667(2)	14.533(3)	27.374(3)	10.6840(10)
α (deg)	90	90	80.59(3)	90	90
β (deg)	97.26(3)	97.706(2)	82.05(3)	90	90
γ (deg)	90	90	81.85(3)	90	90
V (Å^3)	1519.2(5)	3016.6(7)	806.7(3)	3890.0(8)	1944.3(3)
Z	4	8	2	8	4
T (K)	293(2)	298(2)	293(2)	298(2)	298(2)
D_{calcd} (g·cm^{-3})	2.021	1.796	1.961	2.299	1.979
μ (mm^{-1})	3.160	4.102	2.979	5.374	6.310
F(000)	920	1616	476	2544	1128
θ for data collection (deg)	3.03 to 25.33	2.28 to 25.01	3.02 to 25.35	1.71 to 25.00	2.14 to 25.01
reflections collected/unique	7195/1394	7385/2659	7837/2914	16196/3450	9455/1712
R(int)	0.0317	0.0303	0.0311	0.0876	0.0368
parameters	109	199	226	362	122
GOF on F^2	1.074	1.013	1.080	1.121	1.033
R1, wR2 [$I > 2\sigma(I)$][a]	0.0430, 0.1053	0.0296, 0.0663	0.0598, 0.1582	0.0477, 0.1034	0.0272, 0.0582
R1, wR2 (all data)[a]	0.0487, 0.1090	0.0508, 0.0752	0.0737, 0.1700	0.0864, 0.1337	0.0493, 0.0651
ρ_{fin} (max/min) (e·Å^{-3})	0.627/− 0.559	0.354/− 0.507	0.885/− 1.147	1.126/− 1.442	0.399/− 0.369
	6	**7**	**8**	**9**	**10**
empirical formula	$C_{15}H_{14}N_6Cu_3Br_3$	$C_{16}H_{12}N_8Cu_2$	$C_{14}H_{12}N_6Cu_4Cl_4$	$C_{14}H_{12}N_6Cu_4Br_4$	$C_{16}H_{16}N_6Cu_2Cl_2$
fw	708.67	443.42	660.26	838.10	490.33
cryst syst	triclinic	orthorhombic	monoclinic	monoclinic	orthorhombic
space group	$P\bar{1}$	*Pnma*	*P*2(1)/*n*	*P*2(1)/*n*	*Fddd*
a (Å)	8.4740(10)	14.625(3)	7.2894(15)	7.6910(15)	20.840(2)
b (Å)	10.7340(12)	14.645(2)	16.269(3)	16.509(2)	25.570(2)
c (Å)	11.2700(14)	7.6099(13)	15.829(3)	16.021(2)	28.740(3)
α (deg)	80.8520(10)	90	90	90	90
β (deg)	85.449(2)	90	99.52(3)	102.860(2)	90
γ (deg)	69.0960(10)	90	90	90	90
V (Å^3)	945.18(19)	1629.9(5)	1851.3(7)	1983.1(5)	15315(3)
Z	2	4	4	4	32
T (K)	298(2)	291(2)	293(2)	298(2)	298(2)
D_{calcd} (g·cm^{-3})	2.490	1.807	2.369	2.807	1.701
μ (mm^{-1})	9.699	2.628	5.125	12.305	2.513
F(000)	676	888	1288	1576	7872
θ for data collection (deg)	1.83 to 25.01	3.02 to 25.34	3.10 to 25.35	2.74 to 25.01	1.45 to 25.00
reflections collected/unique	4878/3265	14908/1553	17777/3386	9009/3236	18277/3384
R(int)	0.0280	0.0311	0.0346	0.0892	0.1325
parameters	244	128	243	263	236
GOF on F^2	1.040	1.023	1.080	1.044	1.020
R1, wR2 [$I > 2\sigma(I)$][a]	0.0387, 0.0931	0.0648, 0.1737	0.0502, 0.1054	0.0988, 0.2418	0.0760, 0.1933
R1, wR2 (all data)[a]	0.0553, 0.1018	0.0658, 0.1744	0.0573, 0.1087	0.1170, 0.2600	0.1351, 0.2563
ρ_{fin} (max/min) (e·Å^{-3})	0.858/− 1.111	0.789/− 0.707	1.532/− 1.540	1.978/− 1.712	0.712/− 0.802

[a] $R1 = \Sigma(|F_o| - |F_c|)/\Sigma|F_o|$, $wR2 = [\Sigma w(F_o^2 - F_c^2)^2/ \Sigma w(F_o^2)^2]^{0.5}$.

pounds that may not be accessible using the conventional method, but it can also enhance the metal−ligand interactions, thereby promoting crystal growth because the nature and temperature of the hydrothermal or solvothermal fluid can be varied over a wide range. The assembly of a number of rigid ligands and metal salts produced various polymeric solids with new coordination modes, beautiful architectures, and interesting topologies.[20] However, to date, the self-assembly reactions of metal ions and flexible α,*ω*-bis(benzotriazole)alkane ligands that have been described have all adopted the conventional solution method under ambient conditions.[16] In view of the insolubility of copper(I) halides and pseudohalides in common solvents,[21] we investigated the potential of hydro(solvo)thermal reactions of CuX (X = Cl, Br, I, or CN) and flexible bis(benzotriazole)alkane ligands at higher temperatures and with longer reaction times. Our successful synthesis of hybrid solids **1**−**10** proves that bis(benzotriazole)alkane ligands are stable under these conditions.

For complexes **1**, **3**, and **10**, the initial metal source is $CuCl_2 \cdot 2H_2O$, but the ultimate oxidation state of the copper atoms in these compounds is unambiguously +1, based on the condition of charge neutrality, the crystal color, and the coordination environment. Thus, it is noteworthy that under

(20) (a) Rabenau, A. *Angew. Chem., Int. Ed. Engl.* **1985**, *24*, 1026. (b) Feng, S.; Xu, R. *Acc. Chem. Res.* **2001**, *34*, 239. (c) Lu, J. Y. *Coord. Chem. Rev.* **2003**, *246*, 327, and references therein.

(21) (a) Chesnut, D. J.; Zubieta, J. *Chem. Commun.* **1998**, 1707. (b) Chesnut, D. J.; Kusnetzow, A.; Birge, R. R.; Zubieta, J. *Inorg. Chem.* **1999**, *38*, 2663. (c) Teichert, O.; Sheldrick, W. S. *Z. Anorg. Allg. Chem.* **2000**, *626*, 2196. (d) Li, D.; Wu, T. *Inorg. Chem.* **2005**, *44*, 1175. (e) Wu, T.; Li, D.; Alg, S. W. *CrystEngComm.* **2005**, *7*, 514.

Table 2. Selected Bonded Lengths (Å) and Angles (deg) for Complexes **1**−**7**

complex **1**							
Cu(1)−N(1)	2.037(3)	Cu(1)−Cl(1)	2.3540(13)	N(3)−Cu(1)−N(1)	107.29(13)	N(3)−Cu(1)−Cl(1)	117.10(10)
Cu(1)−N(3)	2.020(3)	Cu(1)−Cl(1)#1	2.4254(15)	N(1)−Cu(1)−Cl(1)	117.23(11)	N(3)−Cu(1)−Cl(1)#1	110.62(11)
symmetry codes: #1 $-x$, y, $-z + 3/2$				N(1)−Cu(1)−Cl(1)#1	108.71(11)	Cl(1)−Cu(1)−Cl(1)#1	95.04(5)
complex **2**							
Cu(1)−N(3)	2.040(3)	Cu(1)−Br(1)	2.4578(6)	N(3)−Cu(1)−N(4)	111.91(10)	N(3)−Cu(1)−Br(1)#1	107.37(8)
Cu(1)−N(4)	2.075(3)	Cu(1)−Br(1)#1	2.5355(6)	N(3)−Cu(1)−Br(1)	109.03(7)	N(4)−Cu(1)−Br(1)#1	107.88(7)
symmetry codes: #1 $-x + 1$, $-y + 1$, $-z$				N(4)−Cu(1)−Br(1)	111.88(7)	Br(1)−Cu(1)−Br(1)#1	108.62(2)
complex **3**							
Cu(1)−N(1)	1.824(4)	Cu(2)−N(4)	1.794(4)	N(1)−Cu(1)−Cl(1)	115.71(13)	N(4)−Cu(2)−Cl(2)	99.55(13)
Cu(1)−Cl(1)	1.9955(15)	Cu(2)−Cl(2)	2.2431(17)	N(1)−Cu(1)−N(2)#1	114.30(19)	N(4)−Cu(2)−Cl(2)#2	106.33(18)
Cu(1)−N(2)#1	2.307(5)	Cu(2)−Cl(2)#2	2.681(2)	Cl(1)−Cu(1)−N(2)#1	110.49(13)	Cl(2)−Cu(2)−Cl(2)#2	109.51(7)
symmetry codes: #1 $-x + 1$, $-y + 1$, $-z + 1$; #2 x + 1, y, z							
complex **4**							
Cu(1)−N(1)	2.024(11)	Cu(2)−N(4)	2.026(12)	N(1)−Cu(1)−I(2)	111.6(5)	N(4)−Cu(2)−I(2)#1	112.3(5)
Cu(1)−I(1)	2.659(3)	Cu(2)−I(1)	2.851(2)	N(1)−Cu(1)−I(1)	110.9(5)	N(4)−Cu(2)−I(1)#1	112.5(5)
Cu(1)−I(2)	2.651(3)	Cu(2)−I(1)#1	2.640(2)	I(2)−Cu(1)−I(1)	109.59(7)	I(2)#1−Cu(2)−I(1)#1	110.91(8)
Cu(1)−I(2)#1	2.800(2)	Cu(2)−I(2)#1	2.628(2)	N(1)−Cu(1)−I(2)#1	93.5(3)	N(4)−Cu(2)−I(1)	91.3(3)
symmetry codes: #1 x, $-y$, $-z + 3/2$				I(2)−Cu(1)−I(2)#1	115.23(9)	I(2)#1−Cu(2)−I(1)	114.46(8)
				I(1)−Cu(1)−I(2)#1	115.13(9)	I(1)#1−Cu(2)−I(1)	114.08(8)
complex **5**							
Cu(1)−N(3)	2.006(3)	Cu(1)−Br(1)	2.5658(7)	N(3)−Cu(1)−Br(1)#1	113.63(9)	Br(1)#1−Cu(1)−Br(1)#2	110.68(2)
Cu(1)−Br(1)#1	2.5074(7)	Cu(1)−Br(1)#2	2.5119(7)	N(3)−Cu(1)−Br(1)#2	110.74(9)	Br(1)#1−Cu(1)−Br(1)	107.02(2)
symmetry codes: #1 $-x + 1/2$, $-y + 1/2$, z; #2 $-y + 1/2$, x, $-z + 5/2$				N(3)−Cu(1)−Br(1)	105.68(8)	Br(1)#2−Cu(1)−Br(1)	108.79(2)
complex **6**							
Cu(1)−N(1)	2.032(5)	Cu(2)−Br(2)	2.4948(11)	N(1)−Cu(1)−Br(3)	122.13(14)	Br(2)−Cu(2)−Br(2)#1	105.45(4)
Cu(1)−Br(1)	2.6561(12)	Cu(2)−Br(2)#1	2.5243(12)	N(1)−Cu(1)−Br(2)	108.47(14)	Br(1)−Cu(2)−Br(2)#1	106.25(4)
Cu(1)−Br(2)	2.4868(12)	Cu(3)−N(3)#2	2.015(5)	Br(3)−Cu(1)−Br(2)	110.34(4)	N(3)#2−Cu(3)−Br(3)	125.77(15)
Cu(1)−Br(3)	2.4666(11)	Cu(3)−Br(1)	2.5421(13)	N(1)−Cu(1)−Br(1)	111.47(14)	N(3)#2−Cu(3)−Br(1)	104.63(15)
Cu(2)−N(4)	2.008(5)	Cu(3)−Br(3)	2.4192(11)	Br(3)−Cu(1)−Br(1)	103.84(4)	Br(3)−Cu(3)−Br(1)	108.78(4)
Cu(2)−Br(1)	2.5223(12)	Cu(3)−Br(3)#3	2.6174(12)	Br(2)−Cu(1)−Br(1)	97.85(4)	N(3)#2−Cu(3)−Br(3)#3	102.89(15)
symmetry codes: #1 $-x + 1$, $-y + 1$, $-z + 1$; #2 $x - 1$, y, z; #3 $-x + 1$, $-y + 1$, $-z$				N(4)−Cu(2)−Br(2)	120.40(14)	Br(3)−Cu(3)−Br(3)#3	100.78(4)
				Br(2)−Cu(2)−Br(1)	101.27(4)	Br(1)−Cu(3)−Br(3)#3	114.18(4)
				N(4)−Cu(2)−Br(2)#1	102.11(15)		
complex **7**							
Cu(1)−N(4)	1.937(10)	Cu(2)−N(5)#3	1.917(10)	N(4)−Cu(1)−C(3)	121.7(4)	N(1)#1−Cu(1)−N(1)#2	102.2(3)
Cu(1)−C(3)	1.976(8)	Cu(2)−C(2)	1.948(7)	N(4)−Cu(1)−N(1)#1	112.3(2)	N(5)#3−Cu(2)−C(2)	122.2(3)
Cu(1)−N(1)#1	2.099(5)	Cu(2)−N(2)	2.173(5)	C(3)−Cu(1)−N(1)#1	103.1(2)	N(5)#3−Cu(2)−N(2)	110.8(2)
symmetry codes: #1 $x + 1/2$, y, $-z + 3/2$; #2 $x + 1/2$, $-y + 1/2$, $-z + 3/2$; #3 $x - 1/2$, $-y + 1/2$, $-z + 1/2$; #4 x, $-y + 1/2$, z						C(2)−Cu(2)−N(2)	104.6(2)
						N(2)−Cu(2)−N(2)#4	101.6(3)

Table 3. Selected Bonded Lengths (Å) and Angles (deg) for Complexes **8**−**10**

complex **8**

Cu(1)−N(3)	1.989(4)	Cu(3)−N(1)	2.010(4)	N(3)−Cu(1)−Cl(4)	113.97(13)	Cl(1)−Cu(2)−Cl(2)#1	101.90(6)
Cu(1)−Cl(2)	2.3659(16)	Cu(3)−Cl(3)	2.2131(16)	N(3)−Cu(1)−Cl(2)	117.85(13)	N(1)−Cu(3)−Cl(3)	129.64(13)
Cu(1)−Cl(3)	2.5102(16)	Cu(3)−Cl(1)#2	2.2867(17)	N(3)−Cu(1)−Cl(3)	115.95(13)	N(1)−Cu(3)−Cl(1)#2	106.76(13)
Cu(1)−Cl(4)	2.2731(16)	Cu(4)−N(4)#3	1.990(4)	Cl(2)−Cu(1)−Cl(3)	93.93(6)	Cl(3)−Cu(3)−Cl(1)#2	119.54(7)
Cu(2)−N(2)	1.956(4)	Cu(4)−Cl(2)	2.3249(16)	Cl(4)−Cu(1)−Cl(2)	106.47(6)	N(4)#3−Cu(4)−Cl(2)	118.05(13)
Cu(2)−Cl(1)	2.5862(17)	Cu(4)−Cl(3)	2.4136(17)	Cl(4)−Cu(1)−Cl(3)	106.40(6)	N(4)#3−Cu(4)−Cl(3)	123.35(14)
Cu(2)−Cl(2)#1	2.6313(17)	Cu(4)−Cl(1)#4	2.562(2)	N(2)−Cu(2)−Cl(4)	144.59(14)	Cl(2)−Cu(4)−Cl(3)	97.59(6)
Cu(2)−Cl(4)	2.2022(16)			N(2)−Cu(2)−Cl(1)	98.30(13)	N(4)#3−Cu(4)−Cl(1)#4	105.07(14)
				Cl(4)−Cu(2)−Cl(1)	109.80(6)	Cl(2)−Cu(4)−Cl(1)#4	111.93(6)
				N(2)−Cu(2)−Cl(2)#1	95.68(13)	Cl(3)−Cu(4)−Cl(1)#4	99.49(6)
				Cl(4)−Cu(2)−Cl(2)#1	99.02(6)		

symmetry codes: #1 $x-1, y, z$; #2 $-x, -y+2, -z+1$; #3 $-x+1/2, y+1/2, -z+1/2$; #4 $x+1, y, z$

complex **9**

Cu(1)−N(1)	1.946(19)	Cu(2)−Br(3)	2.445(3)	N(1)−Cu(1)−Br(1)	133(2)	Br(2)−Cu(2)−Br(1)	100.66(10)
Cu(1)−Br(1)	2.44(3)	Cu(3)−N(5)	2.055(15)	N(1)−Cu(1)−Br(2)	118(3)	N(5)−Cu(3)−Br(1)	115.0(4)
Cu(1)−Br(2)	2.65(7)	Cu(3)−Br(1)	2.418(3)	Br(1)−Cu(1)−Br(2)	99.1(13)	N(5)−Cu(3)−Br(4)#2	102.6(4)
Cu(1)−Br(3)	2.69(4)	Cu(3)−Br(4)#2	2.509(3)	N(1)−Cu(1)−Br(3)	109.4(18)	Br(1)−Cu(3)−Br(4)#2	105.18(11)
Cu(1′)−N(1)	1.97(3)	Cu(3)−Br(4)	2.518(3)	Br(1)−Cu(1)−Br(3)	93.9(15)	N(5)−Cu(3)−Br(4)	103.4(4)
Cu(1′)−Br(1)	2.320(17)	Cu(4)−N(6)#2	1.987(15)	Br(2)−Cu(1)−Br(3)	95.5(9)	Br(1)−Cu(3)−Br(4)	115.49(12)
Cu(1′)−Br(3)	2.47(4)	Cu(4)−Br(2)	2.404(3)	N(1)−Cu(1′)−Br(1)	138.9(17)	Br(4)#2−Cu(3)−Br(4)	114.68(11)
Cu(2)−N(3)#1	1.953(14)	Cu(4)−Br(4)	2.539(3)	N(1)−Cu(1′)−Br(3)	117.8(9)	N(6)#2−Cu(4)−Br(2)	134.1(4)
Cu(2)−Br(1)	2.553(3)	Cu(4)−Br(3)#3	2.646(3)	Br(1)−Cu(1′)−Br(3)	103.3(13)	N(6)#2−Cu(4)−Br(4)	104.3(4)
Cu(2)−Br(2)	2.478(3)			N(3)#1−Cu(2)−Br(3)	121.2(4)	Br(2)−Cu(4)−Br(4)	111.14(11)
				N(3)#1−Cu(2)−Br(2)	110.9(5)	N(6)#2−Cu(4)−Br(3)#3	98.7(4)
				Br(3)−Cu(2)−Br(2)	106.79(11)	Br(2)−Cu(4)−Br(3)#3	95.67(10)
				N(3)#1−Cu(2)−Br(1)	117.4(4)	Br(4)−Cu(4)−Br(3)#3	110.05(12)
				Br(3)−Cu(2)−Br(1)	97.38(10)		

symmetry codes: #1 $-x+1/2, y-1/2, -z+3/2$; #2 $-x+1, -y, -z+1$; #3 $x+1, y, z$

complex **10**

Cu(1)−N(3)	1.966(7)	Cu(2)−N(6)	1.971(7)	N(3)−Cu(1)−Cl(2)	114.3(2)	N(6)−Cu(2)−Cl(1)#1	120.4(2)
Cu(1)−Cl(2)	2.396(3)	Cu(2)−Cl(1)#1	2.354(3)	N(3)−Cu(1)−Cl(1)	114.0(2)	N(6)−Cu(2)−Cl(2)	113.8(2)
Cu(1)−Cl(1)	2.420(3)	Cu(2)−Cl(2)	2.407(3)	Cl(2)−Cu(1)−Cl(1)	107.19(10)	Cl(1)#1−Cu(2)−Cl(2)	106.66(9)
Cu(1)−Cl(2)#1	2.471(3)	Cu(2)−Cl(1)	2.523(3)	N(3)−Cu(1)−Cl(2)#1	115.7(2)	N(6)−Cu(2)−Cl(1)	111.7(2)
				Cl(2)−Cu(1)−Cl(2)#1	101.58(9)	Cl(1)#1−Cu(2)−Cl(1)	98.54(9)
				Cl(1)−Cu(1)−Cl(2)#1	102.66(10)	Cl(2)−Cu(2)−Cl(1)	103.62(10)

symmetry codes: #1 $x, -y+5/4, -z+9/4$

Table 4. Summary of Structural Characteristics of Complexes **1**−**10**

complex	coordination geometry [a]	bridging modes of **L**	centroid−centroid distances[b] (Å)	inorganic subunits	dimension
$[CuCl]_2$**L1** (**1**)	tet, $\{CuN_2Cl_2\}$	μ_4	3.76	$\{Cu_2Cl_2\}$ clusters	1-D
[CuBr]**L2** (**2**)	tet, $\{CuN_2Br_2\}$	μ_2	3.69	$\{Cu_2Br_2\}$ clusters	1-D
$[CuCl]_2$**L3** (**3**)	tri, $\{CuN_2Cl\}$ pyr, $\{CuNCl_2\}$	μ_3	4.03	$\{CuCl\}_n$ single chains	1-D
$[CuI]_2$**L4** (**4**)	tet, $\{CuNI_3\}(\times 2)$	μ_2	3.69, 4.02	$\{Cu_4I_4\}$ cubane clusters	1-D
$[CuBr]_2$**L4** (**5**)	tet, $\{CuNBr_3\}$	μ_2	3.82	$\{Cu_4Br_4\}$ cubane clusters	2-D
$[CuBr]_3$**L5** (**6**)	tet, $\{CuNBr_3\}$ $(\times 3)$	μ_3	3.94	$\{Cu_3Br_3\}_n$ ladderlike chains	2-D
$[CuCN]_2$**L1** (**7**)	tet,$\{CuN_2(CN)_2\}$ $(\times 2)$	μ_4	3.71	$\{Cu(CN)\}_n$single chains	3-D
$[CuCl]_4$**L2** (**8**)	tet, $\{CuNCl_3\}$ $(\times 3)$ tri, $\{CuNCl_2\}$	μ_4	3.63, 4.14	$\{Cu_4Cl_4\}_n$ ribbons	3-D
$[CuBr]_4$**L2** (**9**)	tet, $\{CuNBr_3\}$ $(\times 4)$	μ_4	4.00, 4.12	$\{Cu_4Br_4\}_n$ ribbons	3-D
$[CuCl]_2$**L4** (**10**)	tet, $\{CuNCl_3\}$	μ_2	3.83, 3.87	$\{Cu_4Cl_4\}$ cubane clusters	3-D

[a] Key: tet, tetrahedral; tri, trigonal; pyr, pyramidal. [b] Center-to-center distances between benzotriazole rings for $\pi-\pi$ stacking interactions.

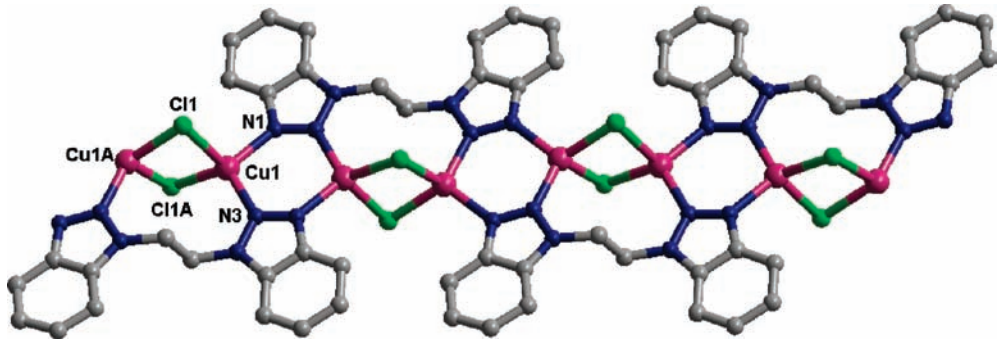

Figure 1. View of the 1-D chain structure in **1**.

hydrothermal conditions bis(benzotriazole)alkane species behave typically not only as ligands but also as reducing agents in the presence of Cu(II). This characteristic is not unusual[22] and obviously results from the combination of the reactive oxidation−reduction potentials of the copper ions and the organonitrogen ligands, as well as the specific hydrothermal conditions. In the preparation of **7**, we used $K_3Fe(CN)_6$ as a precursor instead of KCN to provide CN^-, on the basis of the following considerations: (1) Free cyanide might be released from the dissociation of ferricyanide anions under hydrothermal conditions. (2) The slow release of CN^- might play an important role in the formation of various compounds. (3) Cyanide-bridged iron(II)−copper(I) dimetallic compounds might be obtained under appropriate conditions.[23] Moreover, the role of temperature in determining the architectures of the products was also observed. The self-assembly of CuBr and **L2** gives prism-shaped crystals of **2** at 160 °C, whereas at a higher temperature of 180 °C, block-like crystalline **9** is obtained instead of **2**.

Description of Crystal Structures. 1-D Complexes of $\{[CuCl]_2(L1)\}_n$ (1), $\{[CuBr](L2)\}_n$ (2), $\{[CuCl]_2(L3)\}_n$ (3), and $\{[CuI]_2(L4)\}_n$ (4). Complex **1** shows an infinite 1-D chain structure constructed from $[Cu_2Cl_2]$ binuclear inorganic units and μ_4-bridging 1,2-bis(benzotriazol-1-yl)ethane (**L1**). As shown in Figure 1, the Cu(1) center is a four-coordinated distorted tetrahedral coordination geometry defined by two nitrogen atoms from two **L1** ligands and two chloride atoms. The Cu−N and Cu−Cl bond lengths are 2.037(3)−2.020(3) and 2.3540(13)−2.4254(15) Å, respectively (Table 3), and the corresponding bond angles are in the range of 95.04(5)−117.23(11)° (Table 2). Two Cu(I) atoms are bridged by two μ_2-Cl's to form the rhomboid [Cu−Cl−Cu−Cl] binuclear units. Adjacent binuclear units are linked by 1,2-bis(benzotriazol-1-yl)ethane ligands using an unprecedented μ_4-bridging mode to form the infinite organic−inorganic hybrid chain of complex **1**. It should be noted that the bridging mode of benzotriazole in **L1** (N_2,N_3-bridging mode) between two adjacent $[Cu_2Cl_2]$ units is similar to the N_1,N_2-bridging mode of 1,2,4-triazole ligands, which is first observed in the coordination chemistry of α,ω-bis(benzotriazole)alkane ligands. Thus, two copper atoms are separated by about 3.7 Å, which is less than the distance of 4 Å that is usually found in the metal−1,2,4-triazolate compounds.[10b] Further, the 1-D chains are extended into the final 2-D networks, as depicted in Figure S1 in the Supporting Information, through strong aromatic $\pi-\pi$ stacking interactions between benzotriazole rings from adjacent chains, with a center-to-center distance of about 3.761 Å.

The reaction of CuBr with an asymmetrical 1,2′-isomer of 1,2-bis(benzotriazole)ethane (**L2**) leads to the formation of complex **2** that presents a 1-D chain structure consisting of $[Cu_2Br_2]$ binuclear units and μ_2-bridging organic ligands. As in complex **1**, two μ_2-Br atoms are bound to two adjacent Cu(I) centers, forming a $[Cu_2Br_2]$ parallelogram dimer (Figure 2). The Cu−Br distances of 2.4578(6) and 2.5355(6) Å are within the normal range. However, the Br−Cu−Br and Cu−Br−Cu angles are 108.62(2) and 71.384(17)°, respectively, which indicates that this dimer is highly distorted compared with one-half of the $[Cu_4Br_4]$ cubane core.[24] As a result, the copper atoms are separated

(22) (a) Hagrman, D.; Zubieta, C.; Rose, D. J.; Zubieta, J.; Haushalter, R. C. *Angew. Chem., Int. Ed. Engl.* **1997**, *36*, 873. (b) Hagrman, D.; Zapf, P. J.; Zubieta, J. *Chem. Commun.* **1998**, 1283. (c) Hagrman, D.; Zubieta, J. *Chem. Commun.* **1998**, 2005. (d) LaDuca, R. L., Jr.; Finn, R.; Zubieta, J. *Chem. Commun.* **1999**, 1669. (e) Wu, C. D.; Lu, C. Z.; Zhuang, H. H.; Huang, J. S. *Inorg. Chem.* **2002**, *41*, 5636.

(23) (a) Colacio, E.; Kivekas, R.; Lloret, F.; Sunberg, M.; Varela, J. S.; Bardaji, M.; Laguna, A. *Inorg. Chem.* **2002**, *41*, 5141. (b) Colacio, E.; Debdoubi, A.; Kivekas, R.; Rodriguez, A. *Eur. J. Inorg. Chem.* **2005**, 2860.

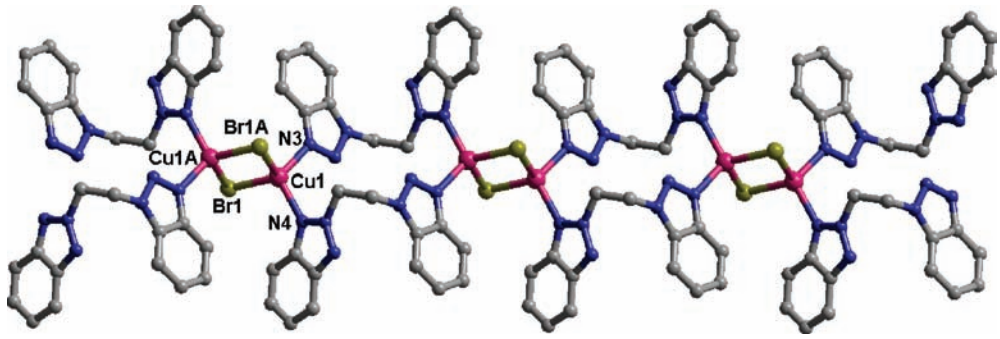

Figure 2. View of the 1-D chain structure in **2**.

by only 2.9138(6) Å, which is slightly longer than the sum of the van der Waals radii (2.80 Å) but is markedly shorter than the distances usually observed in the cubane core, possibly indicating the existence of a weak Cu···Cu interaction. This is different from the 1,1′-isomer (**L1**) in complex **1** since each benzotriazole in **L2** only provides one nitrogen atom to coordinate with the copper(I) center. Thus, the whole **L2** ligand adopts a common μ_2-bridging mode to link the inorganic subunits. The dihedral angle of two benzotriazole rings in one **L2** is 91.9°, and the torsion angle of $N_{benzotriazole}-(C-C)-N_{benzotriazole}$ is 68.3°. Two adjacent $[Cu_2Br_2]$ units are linked by two μ_2-**L2** ligands to generate a 1-D chain structure similar to that of the compound $[(3,4'\text{-bpy})(Br)Cu^{I}]_n$.[25] Just like complex **1**, the strong aromatic $\pi-\pi$ stacking interactions between benzotriazole rings (3.692 Å) from adjacent chains extend the 1-D chains into the 2-D hybrid supramolecular structure of complex **2** (Figure S2 in theSupporting Information).

To further investigate the influence of the alkane length on the hybrid structure, 1,3-bis(benzotriazole)propane (**L3**) was reacted with $CuCl_2$ under the same conditions as **1**. Consequently, **3**, which features a 1-D ribbon structure, was obtained. As shown in Figure 3a, there exist two crystallographically independent three-coordinated Cu(I) centers. One terminal chloride atom and two nitrogen atoms from two different **L3** ligands are coordinated to a Cu(1) atom to form a trigonal geometry, given the distances Cu(1)−Cl(1) = 1.9955(15) Å, Cu(1)−N(1) = 1.824(4) Å, and Cu(1)−N(2) = 2.307(5) Å, respectively. The corresponding bond angles around Cu(1) are in the range of 110.49(13)−115.71(13)°, which indicates that the Cu(1) center is slightly deviated (by 0.5581(9) Å) from the trigonal plane defined by the three donor atoms. The bridging mode of benzotriazole between two adjacent Cu(1) atoms in **L3** is similar to that in **L1** in complex **1**, which leads to the formation of a $[Cu_2N_4]$ six-membered ring and separates the two copper atoms by about 3.5 Å. The coordinate environment around Cu(2) is completed by one nitrogen atom from **L3** and two chloride atoms, with the distances Cu(2)−N(4) = 1.794(4) Å, Cu(2)−Cl(2) = 2.2431(17) Å, and Cu(2)−Cl(2A) = 2.681(2) Å, respectively. The Cu(2) atom is deviated from the [Cl−N−Cl] trigon by about 0.91 Å, generating a $[CuNCl_2]$ pyramid with bond angles ranging from 99.55(13) to 109.51(7)°. Each Cl(2) acts as a μ_2-ligand linking two Cu(2) atoms to form a 1-D [Cu(2)Cl] inorganic chain. Further, two [Cu(2)Cl] chains are linked by the binuclear Cu(1) subunits through 1,3-bis(benzotriazole)propane (**L3**) ligands to give the novel hybrid ribbon structure of complex **3**, as depicted in Figure 3b. Furthermore, the adjacent chains are connected through weak C−H···Cl hydrogen bonding interactions. Thus, a 2-D supramolecular hybrid network is formed via both coordinating and hydrogen bond interactions (Figure S3 in the Supporting Information).

Complex **4** crystallizes in the chiral space group *P*4(1)22 and shows an unprecedented 1-D hybrid chain structure consisting of a Cu_4I_4 cubane subunit, one *R*-**L4** ligand and one *L*-**L4** ligand (Figure 4a). Similar to those of other reported Cu_4I_4 tetramer units,[26] each Cu^+ or I^- links three neighboring I^-s or Cu^+s to form a distorted cubane unit. Two independent copper atoms are both tetrahedrally coordinated by three I^-s and a nitrogen from the benzotriazole of the **L4** ligand with Cu−I and Cu−N distances of 2.628(2)−2.851(2) and 2.024(11)−2.026(12) Å, respectively. The Cu−Cu distances are in the range of 2.6345(51)−2.7279(48) Å, which are comparable to those found in other structurally characterized $Cu_4I_4L_4$ complexes (L = the nitrogen-containing ligand).[26a] Each cubane-like Cu_4I_4 unit is connected with two adjacent units via four μ_2-**L4** ligands (Figure 4a), and this connectivity generates a unique 1-D chain structure. Interestingly, the **L4** ligands located on the two sides of the Cu_4I_4 tetramer are enantiomers. Moreover, the 1-D hybrid chains are extended into a 2-D network, as depicted in Figure 4b, through weak aromatic $\pi-\pi$ stacking interactions between benzotriazole rings from adjacent chains (parallel stacking with centroid−centroid distances of 4.0 Å). Finally, the 2-D nets are further packed into a 3-D supramolecular architecture through strong aromatic $\pi-\pi$ stacking interactions between benzotriazole rings from adjacent 2-D nets, with a center-to-center distance of

(24) (a) Churchill, M. R.; DeBoer, B. G.; Mendak, S. J. *Inorg. Chem.* **1975**, *14*, 2041. (b) Goel, R. G.; Beauchamp, A. L. *Inorg. Chem.* **1983**, *22*, 395. (c) Barron, P. F.; Dyason, J. C.; Engelhardt, L. M.; Healy, P. C.; White, A. H. *Inorg. Chem.* **1984**, *23*, 3766. (d) Dyason, J. C.; Healy, P. C.; Engelhardt, L. M.; Pakawatchai, C.; Patrick, V. A.; Raston, C. L.; White, A. H. *J. Chem. Soc., Dalton Trans.* **1985**, 831. (e) Engelhardt, L. M.; Healy, P. C.; Kildea, J. D.; White, A. H. *Aust. J. Chem.* **1989**, *42*, 107.

(25) Fun, H. K.; Raj, S. S.; Xiong, R. G.; Zuo, J. L.; Yu, Z.; Zhu, X. L.; You, X. Z. *J. Chem. Soc., Dalton Trans.* **1999**, 1711.

(26) (a) Vitale, M.; Ford, P. C. *Coord. Chem. Rev.* **2001**, *219-221*, 3, and references therein. (b) Vega, A.; Saillard, J. Y. *Inorg. Chem.* **2004**, *43*, 4012. (c) Sarkar, M.; Biradha, K. *Chem. Commun.* **2005**, 2229. (d) Hu, S.; Tong, M. L. *Dalton Trans.* **2005**, 1165. (e) Zhai, Q. G.; Lu, C. Z.; Chen, S. M.; Xu, X. J.; Yang, W. B. *Inorg. Chem. Commun.* **2006**, *9*, 819.

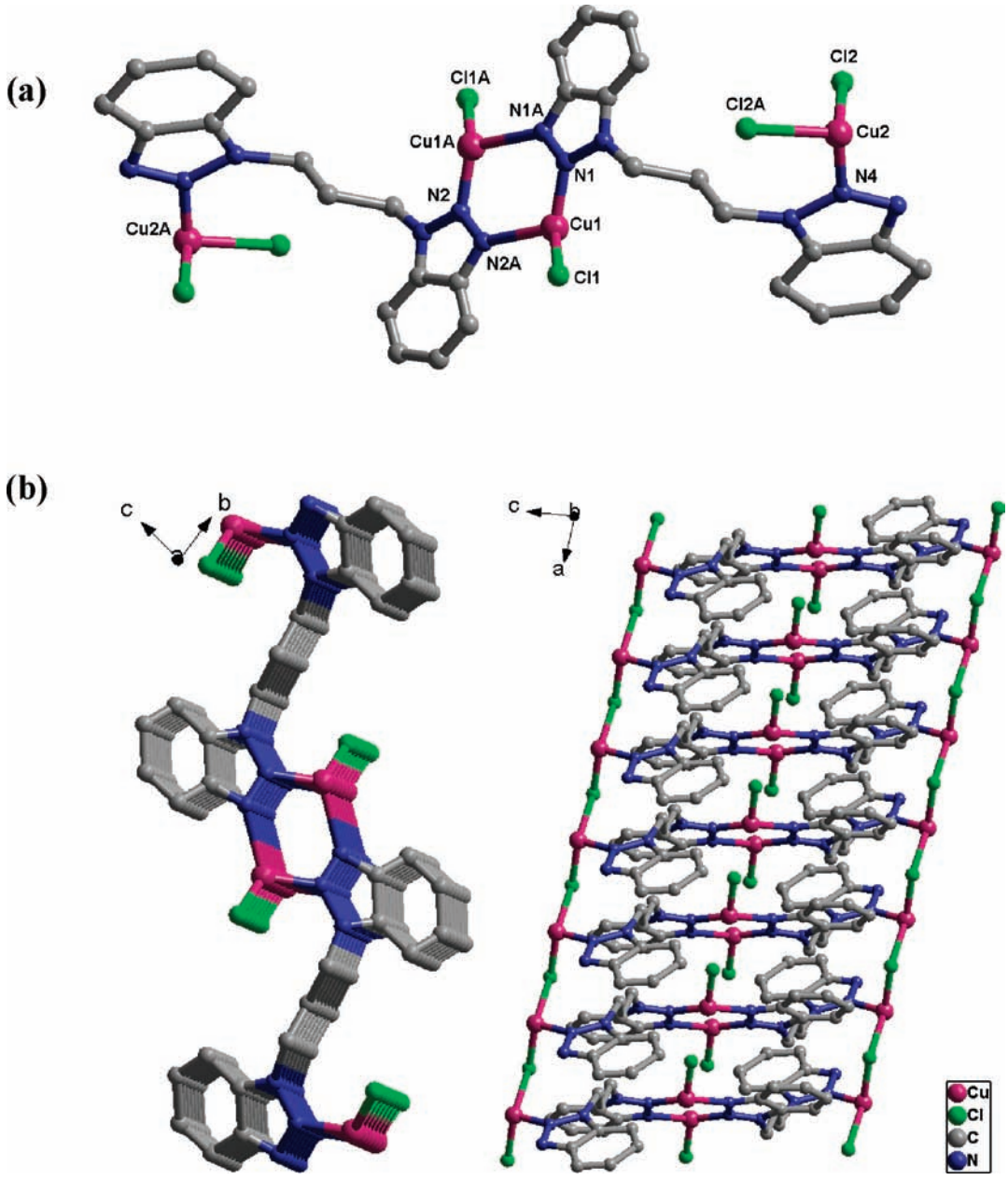

Figure 3. (a) View of the coordination environment of the copper atoms and (b) 1-D ribbonlike hybrid structure viewed from the *a*- and *b*-axis directions for **3**.

3.6897(3) Å. These 2-D nets are packed in a unique ABCBA mode, as depicted in Figure 4b, and this packing mode generates a 1-D channel along the *c*-axis direction with dimensions of about 6 × 6 Å (Figure S4 in the Supporting Information).

2-D Complexes of $\{[CuBr]_2(L4)\}_n$ (5) and $\{[CuBr]_3(L5)\}_n$(6). As shown in Figure 5a, complex **5** can be described as a 2-D (4, 4) net structure with Cu_4Br_4 cubane units as nodes and **L4** ligands as linkers. Just like the Cu_4I_4 tetramer in complex **4**, each Cu^+ or Br^- links three neighboring Br^- or Cu^+ to form a distorted cubane unit. However, there is only one crystallographically unique copper atom that is coordinated by three Br^- and a nitrogen from the **L4** ligand with Cu−Br and Cu−N distances of 2.5074(7)−2.5658(7) and 2.006(3) Å, respectively. The Cu···Cu distances are 2.7681(8) and 2.8314(8) Å, which are markedly shorter than those found in the structurally characterized $Cu_4Br_4L_4$ complexes (L = the phosphorus- or nitrogen-containing ligands).[24] Each cubane Cu_4Br_4 unit is tetrahedrally corner-connected with four adjacent units via four μ_2-**L4** ligands (Figure 5a), and this connectivity generates a 2-D (4, 4) net. The aromatic face-to-face distance of 3.8188(3) Å between the neighboring ligands reveals weak $\pi-\pi$ interactions. Each 2-D sheet is reversed from its neighbors and lies on top of the others along the *c*-axis direction to give an ABAB packing mode (Figure 5b and Figure S5 in the Supporting Information). To our knowledge, **5** is the first coordination polymer structure reported to be constructed from tetrahedral Cu_4Br_4 cubane units.

The architecture of **6** is constructed from **L5** ligands associated with inorganic double-stranded ladder CuBr

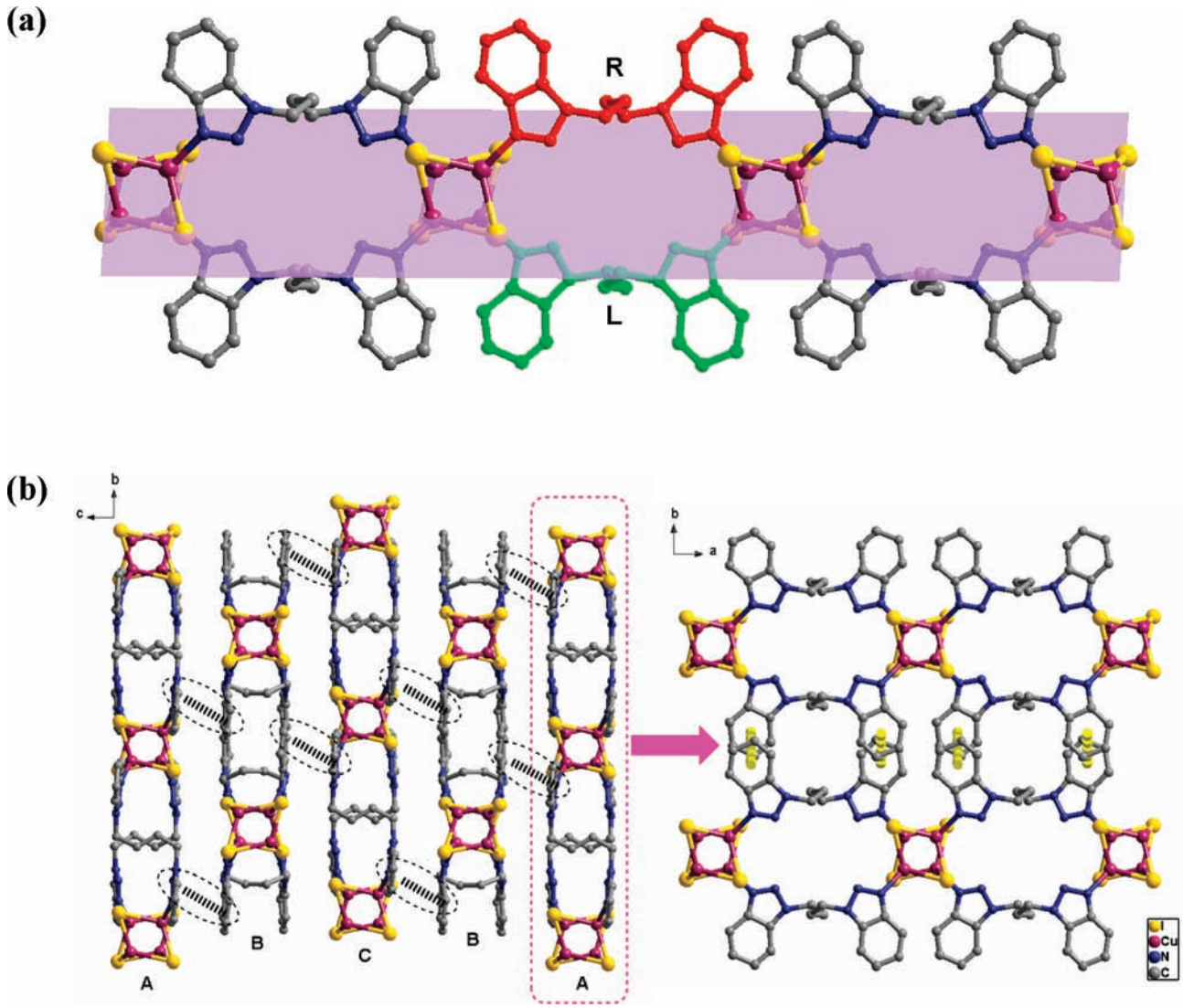

Figure 4. (a) View of the 1-D hybrid chain showing two enantiomers of **L4** in **4**. (b) View of the ABCBA packing diagram along the *a*-axis direction (left) along with one 2-D layer (right).

chains. There exist three crystallographically independent Cu(I) centers in an asymmetric unit. All the Cu(I) ions are tetracoordinated. As illustrated in Figure 6a, each copper atom presents a distorted tetrahedron defined by one nitrogen atom from one **L5** ligand and three bromine atoms with the Cu−Br and Cu−N distances of 2.4192(11)−2.6561(12) and 2.008(5)−2.032(5) Å, respectively. There also exist three independent bromine atoms that all adopt a μ_3-coordinating mode. Each Cu^+ or Br^- links three neighboring Br^- or Cu^+ to form a novel distorted double-stranded ladder chain, as depicted in Figure 6b. Three different $[Cu_2Br_2]$ parallelograms exist in the chain, namely, Cu(1)−Br(1)−Cu(2)−Br(2), Cu(1)−Br(3)−Cu(3)−Br(1), and Cu(3)−Br(3)−Cu(3A)−Br(3A), and the distances between diagonal copper atoms are 2.8942(14), 3.2148(13), and 3.2687(14) Å, respectively. Each **L5** ligand acts as a tridentate bridging ligand, in which one benzotriazole group adopts a μ_2-coordinating mode and the other one is monodentate. Thus, the μ_3-**L5** ligand serves as two types of bridges between Cu(2) and Cu(3) in the $[CuBr]_n$ staircase and adjacent staircases and propagates the 1-D polymeric inorganic chains into infinite 2-D hybrid layers (Figure 6c). Finally, the organic−inorganic layers are extended into the final 3-D supramolecular networks, as depicted in Figure S6 in the Supporting Information, through weak aromatic $\pi-\pi$ stacking interactions between benzotriazole rings from adjacent layers (parallel stacking with centroid−centroid distances of 3.94Å).

3-D Complexes of $\{[CuCN]_2(L1)\}_n$ (7), $\{[CuCl]_4(L2)\}_n$ (8), $\{[CuBr]_4(L2)\}_n$ (9), and $\{[CuCl]_2(L4)\}_n$ (10). The self-assembly of **L1** with CuCN resulted in the formation of the 3-D hybrid architecture of compound **7** that is constructed from 1-D inorganic $[Cu(CN)]_n$ chains connected by **L1** acting as a tetradentate bridging ligand. As shown in Figure 7a, two independent copper centers are both tetracoordinated to two nitrogen atoms from different **L1** ligands (Cu−N = 2.099(5) and 2.173(5) Å) and two N/C atoms from different cyanide groups (Cu−N/C = 1.937(10), 1.917(10), 1.976(8), and 1.948(7) Å). The C−N bond lengths of 1.133(12) and 1.153(12) Å and the Cu−N/C distances of 1.917(10)−1.976(8) Å are comparable to those found in previously reported copper cyanides.[27] The Cu(1) and Cu(2) atoms are bridged by CN^- anions to form infinite S-like inorganic $[Cu(CN)]_n$

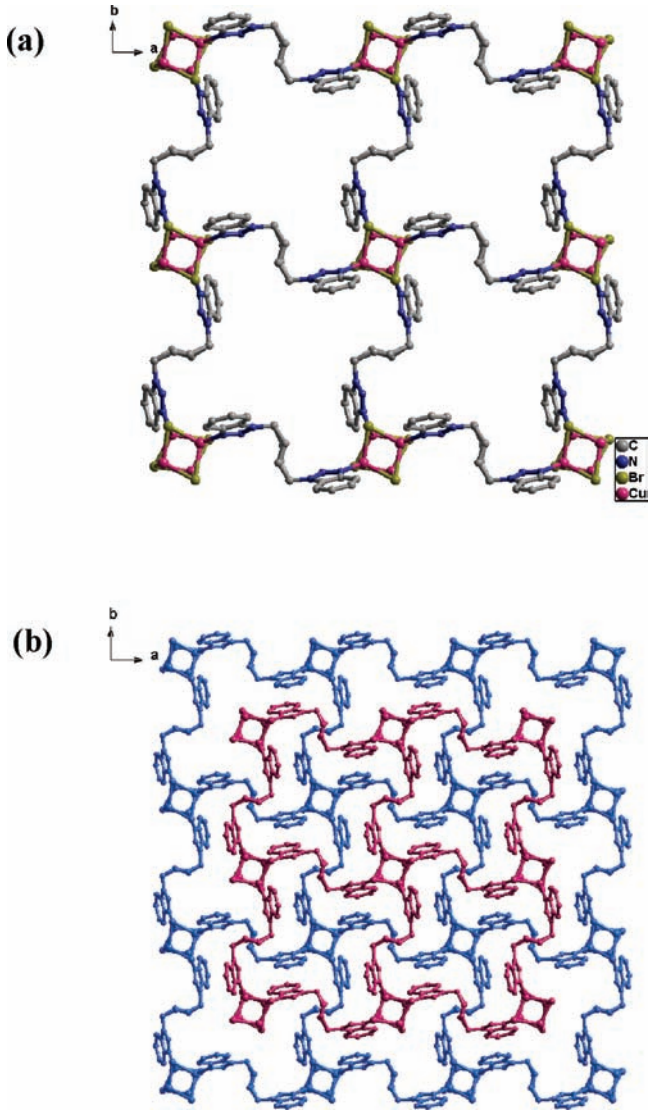

Figure 5. (a) View of the 2-D network in **5** from the *c* axis and (b) packing diagram for **5** viewed from different directions.

chains running along the *a*-axis direction with Cu···Cu separations of 5.0236(18) and 5.0068(19) Å. The C/N−Cu−N/C bond angles (121.7(4) and 122.2(3)°) in this Cu−CN chain are significantly smaller than those (176.7(3)−179.0(5)°) in a low-temperature polymorph,[28] which is due to the bite angle of the **L1** ligand that chelates the copper centers, forming a distorted tetrahedral geometry. Just like the free molecule,[29] each **L1** ligand takes the anticonformation to link four adjacent S-like $[Cu-CN]_n$ chains through four unoccupied nitrogen atoms, as shown in Figure 7b. This connectivity generates the 3-D organic−inorganic hybrid architecture of complex **7** (Figure 7c). To the best of our knowledge, although several coordination polymers with 1,2-bis(benzotriazol-1-yl)ethane (**L1**) have been presented to date,[16d,e] complex **7** is the first 3-D hybrid structure. In our opinion, utilization of the hydrothermal method and the stability of the [Cu−CN] S-like chain formed by μ-CN coordinated to Cu(I) seem to be important determining factors affecting the coordination frameworks of **7**, which overcome the influence of ligands on the metal−organic frameworks.

X-ray structural analysis of **8** and **9** reveals that they are isomorphic, 3-D hybrid structures constructed from unique 1-D inorganic $[Cu_8X_8]_n$ (X = Cl for **8** and X = Br for **9**) ribbons connected by **L2**, which serves as a tetradentate bridging ligand. There exist four crystallographically independent Cu(I) centers in an asymmetric unit of complex **8**. As depicted in Figure 8a, the Cu(1), Cu(2), and Cu(4) atoms all present a distorted tetrahedral geometry coordinated by one nitrogen atom from one **L2** ligand and three chloride atoms with the Cu−Cl and Cu−N distances of 2.2022(16)−2.6313(17) and 1.956(4)−1.990(4) Å, respectively. Moreover, the corresponding bond angles, 93.93(6)−117.85(13)° for Cu(1), 95.68(13)−144.59(14)° for Cu(2), and 97.59(6)−123.35(14)° for Cu(4), show that the $[Cu(2)Cl_3N]$ tetrahedron is highest distorted. Each Cu(3) center presents a planar trigonal geometry coordinated by one nitrogen atom from the **L2** ligand and two chloride atoms (Cu(3)−N(1) = 2.010(4) Å, Cu(3)−Cl(1) = 2.2867(17) Å, Cu(3)−Cl(3) = 2.2131(16) Å). The bond angles around the Cu(3) atom are 106.76(13), 119.54(7), and 129.64(13)°. On the other hand, four independent chloride atoms also exist in this structure with Cl(1), Cl(2), and Cl(3) acting as μ_3-bridges and Cl(4) as a μ_2-bridge, respectively. As shown in Figure 8b, eight copper atoms are first linked by six μ_3-Cl atoms to generate novel $[Cu_8Cl_6]^{2+}$ units that are further bridged by μ_2-Cl(4) atoms to give an unprecedented 1-D inorganic ribbon $[Cu_8Cl_8]$ along the *a*-axis direction. For each $[Cu_8Cl_6]^{2+}$ cationic cluster, there exist four $\{Cu_2Cl_2\}$ and one $\{Cu_4Cl_4\}$ polynuclear rings. Further, the linkage between two cationic clusters generates another $\{Cu_6Cl_6\}$ ring. The Cu···Cu separation distances show remarkable variation, ranging from 2.9817(5) to 6.6917(4) Å in one $[Cu_8Cl_6]^{2+}$ unit and 3.1589(6) to 9.5831(19) Å between two adjacent $[Cu_8Cl_6]^{2+}$ units. As in the case of **L1** in complex **7**, the **L2** ligand acts as a μ_4-bridging ligand through four unoccupied nitrogen atoms. However, each μ_4-**L2** ligand only links two adjacent 1-D inorganic ribbons since three nitrogen atoms are connected to three Cu(I) atoms in one inorganic ribbon. Thus, each $[Cu_8Cl_8]$ inorganic ribbon is linked to four adjacent neighbors by four μ_4-bridging **L2** ligands to give the 3-D organic−inorganic hybrid framework of **8** (Figure 8c and Figure S9 in the Supporting Information).

Although complex **9** is an isomorphic structure of **8**, it presents several distinct structural characteristics. As shown in Figure 9a, four independent Cu(I) atoms are all coordinated to one nitrogen atom from one **L2** ligand and three bromide atoms to form a distorted $[CuBr_3N]$ tetrahedral geometry. It should be noted that the Cu(1) center occupies two positions (Cu(1) and Cu(1′)) to generate a disorder, which is not unusual in polynuclear metal halide com-

(27) (a) Stocker, F. B.; Staeva, T. P.; Rienstra, C. M.; Britton, D. *Inorg. Chem.* **1999**, *38*, 984. (b) Chesnut, D. J.; Plewak, D.; Zubieta, J. *J. Chem. Soc., Dalton Trans.* **2001**, 2567. (c) Hanika-Heidl, H.; Etaiw, S. E. H.; Ibrahim, M. S.; El-din, A. S. B.; Fischer, R. D. *J. Organomet. Chem.* **2003**, *684*, 329. (d) Zhang, X. M.; Fang, R. Q. *Inorg. Chem.* **2005**, *44*, 3955.
(28) Hibble, S. J.; Eversfield, S. G.; Cowley, A. R.; Chippindale, A. M. *Angew. Chem., Int. Ed.* **2004**, *43*, 628.
(29) Li, B. Z.; Zhou, J. H.; Peng, Y. F.; Li, B. L.; Zhang, Y. *J. Mol. Struct.* **2004**, *707*, 187.

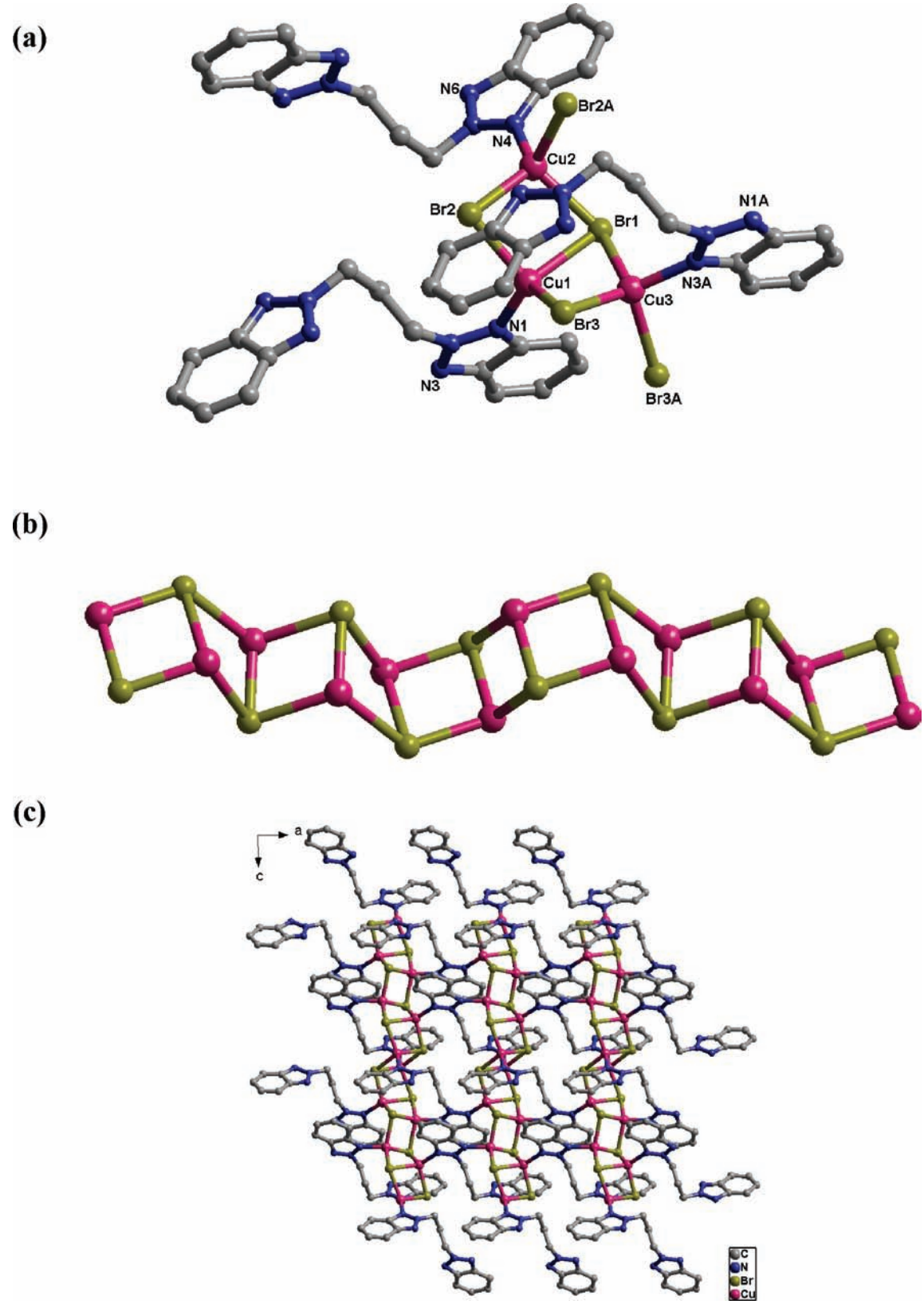

Figure 6. (a) View of the coordination environment of the copper atoms in **6**. (b) View of the 1-D inorganic $[Cu_3Br_3]_n$ chain. (c) 2-D hybrid layer viewed from the *b*-axis direction for **6**.

plexes.[30] The Cu−Br and Cu−N distances are in the ranges of 2.404(3)−2.69(4) and 1.946(19)−2.055(15) Å, respectively. The corresponding bond angles, 93.9(15)−133(2)° for Cu(1), 97.38(10)−121.2(4)° for Cu(2), 102.6(4)−115.49(12)° for Cu(3), and 95.67(10)−134.1(4)° for Cu(4), show that four $[CuBr_3N]$ tetrahedrons are all distorted to some extent. This is different from **8** since four independent bromide atoms, Br(1)−Br(4), all serve as μ_3-bridges to link three Cu(I) atoms.

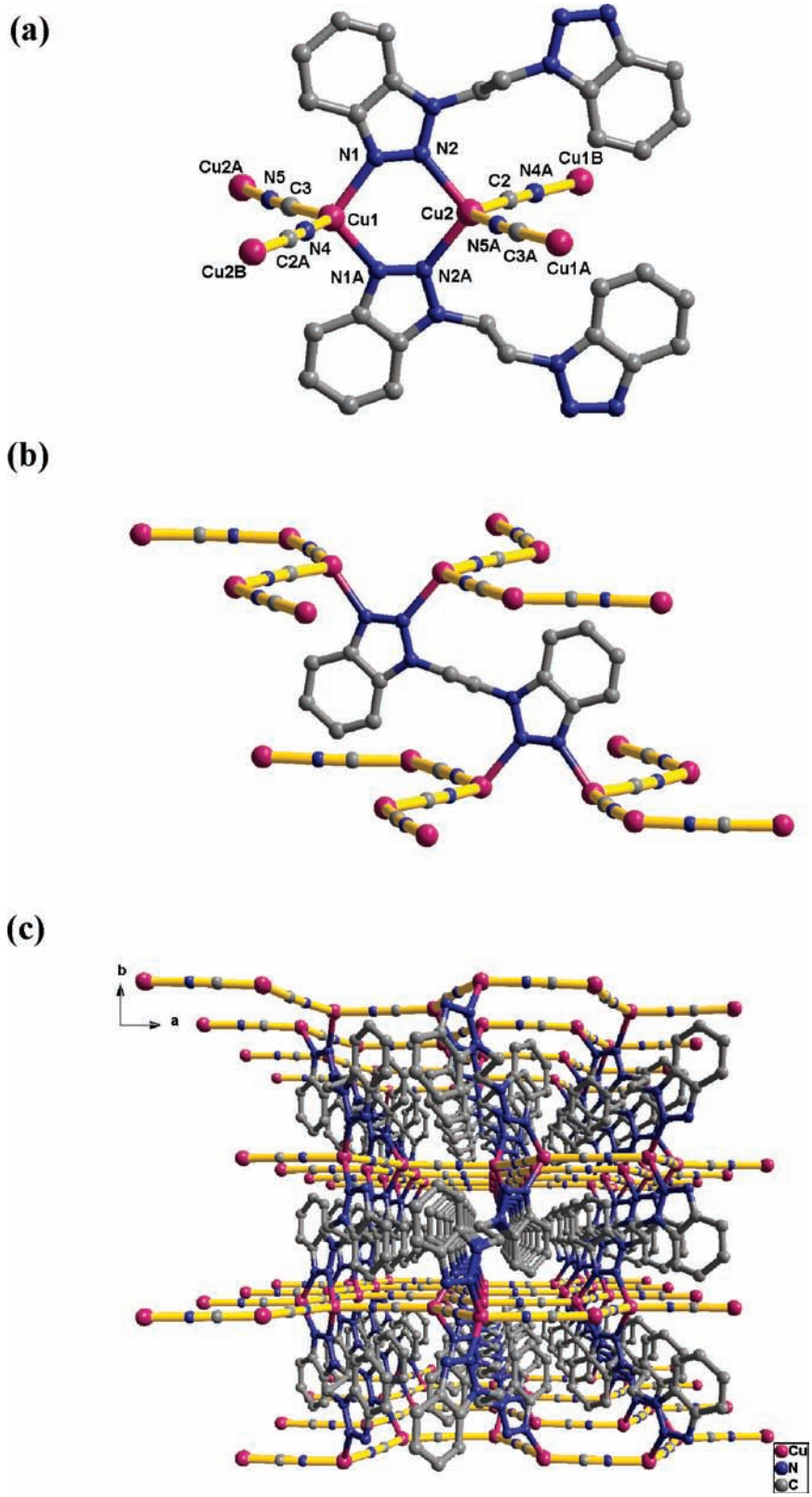

Figure 7. (a) View of the coordination environment of the copper atoms in **7**. (b) View of the linkage between an organic ligand and 1-D inorganic CuCN chains. (c) 3-D hybrid architecture of **7** viewed from the *c*-axis direction.

This connectivity generates a distinct 1-D $[Cu_8Br_8]$ inorganic ribbon along the *a*-axis direction, as shown in Figure 9b. It is noticeable that the basic subunit in this ribbon is not a $\{Cu_8Br_6\}^{2+}$ cation but, rather, is a novel $\{Cu_8Br_8\}$ neutral cluster that contains six μ_3-Br and two μ_2-Br atoms. The adjacent $\{Cu_8Br_8\}$ neutral clusters are connected to each other through two μ_2-Br atoms. In each $\{Cu_8Br_8\}$ neutral cluster, seven $\{Cu_2Br_2\}$ rings and four $\{Cu_3Br_3\}$ rings are observed. Moreover, the linkage between $\{Cu_8Br_8\}$ neutral clusters generates four $\{Cu_6Br_6\}$ rings. The Cu(I) centers in the

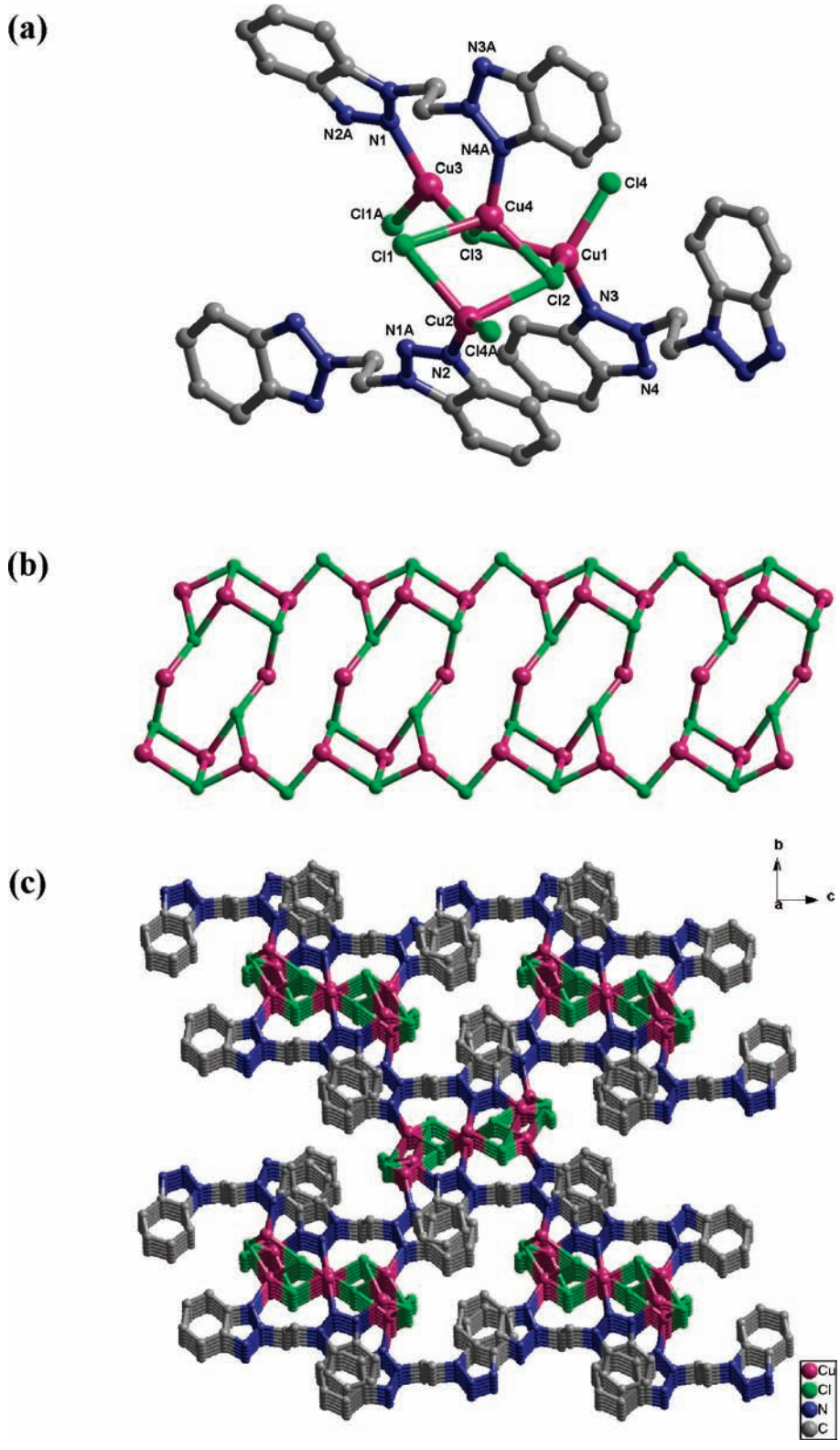

Figure 8. (a) View of the coordination environment of the copper atoms in **8**. (b) View of the 1-D $[Cu_8Br_8]_n$ inorganic ribbon. (c) 3-D hybrid architecture of **8** viewed from the *a*-axis direction.

octanuclear clusters are separated by relatively short distances of 2.6083(42) and 2.7134(45) Å, which are shorter than the sum of their van der Waals radii (2.8 Å). [31] As depicted in Figure S8 in the Supporting Information, each $[Cu_8Br_8]$ inorganic ribbon is linked to four adjacent neighbors via four μ_4-bridging **L2** ligands to form the 3-D hybrid framework of **9**. To the best of our knowledge, the $[Cu_8X_8]_n$ (X = Cl for **8** and X = Br for **9**) ribbonlike chains are the first two examples reported to date and may, thus, represent a novel metal halide skeleton.

Complex **10** exhibits a twofold interpenetrated diamondoid array with Cu_4Cl_4 cubane units as nodes and **L4** ligands as

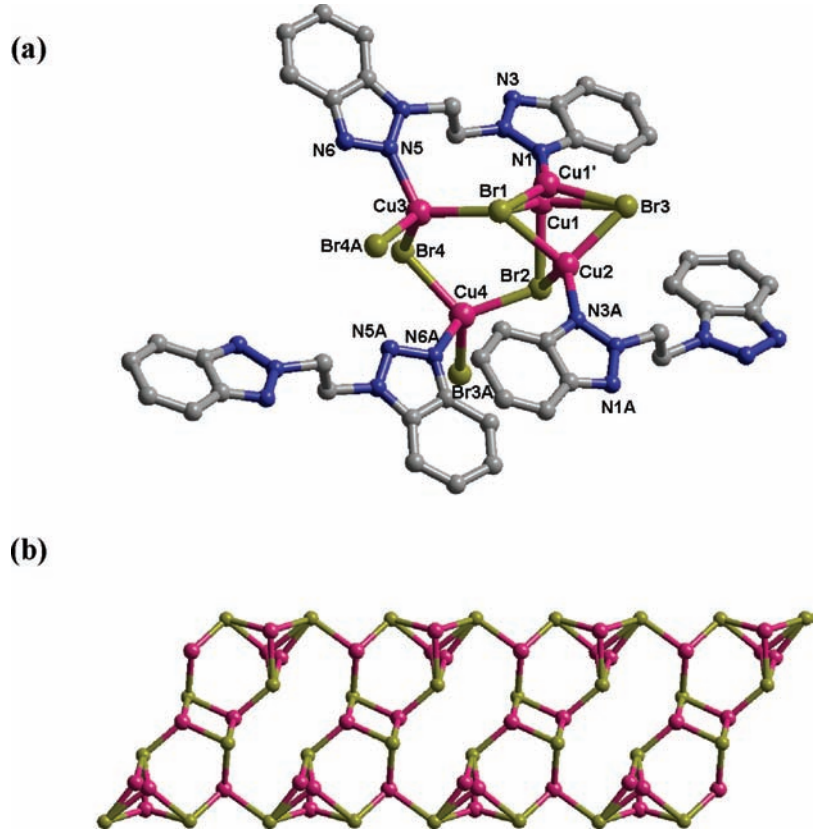

Figure 9. (a) View of the coordination environment of the copper atoms in **9**. (b) View of the 1-D $[Cu_8Br_8]_n$ inorganic ribbon.

linkers. Similar to the cubane clusters in complexes **4** and **5**, each Cu is coordinated primarily by three chloride atoms and one nitrogen atom from **L4**, which define a slightly distorted tetrahedral geometry with Cu−Cl and Cu−N distances of 2.354(3)−2.523(3) and 1.966(7)−1.971(7) Å, respectively. The bond angles around the copper centers are 101.58(9)−115.7(2)° for Cu(1) and 98.54(9)−120.4(2)° for Cu(2). The Cu−Cu distances are in the range of 2.9009(23)−3.0740(22) Å, which are comparable to those found in other structurally characterized $Cu_4Cl_4L_4$ complexes (L = the phosphorus- or nitrogen-containing ligands).[24a,d,e,32] The extension of the structure into a 3-D network is accomplished by tetrahedrally connecting four **L4** ligands to the cubane Cu_4Cl_4 units (Figure 10a). To the best of our knowledge, **10** is the first 3-D net reported to be constructed from the tetrahedral Cu_4Cl_4 cubane units. Topological analysis of **10** reveals that it is a typical diamondoid framework containing large adamantanoid cages. A single cage delimitated by four cyclohexane-like windows in chair conformation is shown in Figure 10b, which exhibits maximum dimensions of 19.23 × 28.74 × 5.57 Å. Because of the spacious nature of the single network, it allows the other identical diamondoid networks to interpenetrate it in a normal mode, giving rise to a twofold interpenetrating diamondoid array (Figure 10c,d and Figure S10 in the Supporting Information). An analysis of the topology of interpenetration according to a recent classification[33] reveals that **10** belongs to Class Ia (i.e., all the interpenetrated nets are generated only by translation). As is often observed in interpenetrated diamondoid network structures, close $\pi-\pi$ contacts occur between benzotriazole rings (parallel stacking with centroid−centroid distances of 3.83 and 3.87 Å) and stabilize the solid-state structures.

Coordination Modes and $\pi-\pi$ Stacking Interactions of the α,ω-Bis(benzotriazole)alkane Ligands. The α,ω-bis(benzotriazole)alkane family represents a series of versatile ligands that can coordinate with metal ions, with one or two benzotriazoles adopting various bridging modes and yielding a variety of coordination frameworks. However, to the best of our knowledge, the previously described metal−organic complexes with α,ω-bis(benzotriazole)alkane as ligands all adopted the conventional solution method under ambient conditions. As a result, only the μ_2-bridging mode has been observed to date.[16] In the present study, we successfully obtained hybrid complexes of various dimensionalities under hydro(solvo)thermal conditions, allowing us to thoroughly investigate the coordination modes of the α,ω-bis(benzotriazole)alkane ligand (Table 4). For **L1** in **1** and **7** and **L2** in **8** and **9**, two benzotriazole groups both act as bidentate

(30) (a) Pfitzner, A. *Chem.—Eur. J.* **2000**, *6*, 1891. (b) Brooks, N. R.; Blake, A. J.; Champness, N. R.; Cooke, P. A.; Hubberstey, P.; Proserpio, D. M.; Wilson, C.; Schröder, M. *J. Chem. Soc., Dalton Trans.* **2001**, 456.
(31) (a) Singh, K.; Long, J. R.; Stavropoulos, P. *J. Am. Chem. Soc.* **1997**, *119*, 2942. (b) Boche, G.; Bosold, F.; Marsch, M.; Harms, K. *Angew. Chem., Int. Ed.* **1998**, *37*, 1684. (c) Kohn, R. D.; Seifert, G.; Pan, Z.; Mahon, M. F.; Kociok-Kohn, G. *Angew. Chem., Int. Ed.* **2003**, *42*, 793.
(32) (a) Churchill, M. R.; Kalra, K. L. *Inorg. Chem.* **1974**, *13*, 1065. (c) Bottcher, H. C.; Graf, M.; Merzweiler, K.; Bruhn, C. *Polyhedron* **1997**, *16*, 3253. (d) Gonzalez, S. D.; Kaur, H.; Zinn, F. K.; Stevens, E. D.; Nolan, S. P. *J. Org. Chem.* **2005**, *70*, 4784.
(33) Blatov, V. A.; Carlucci, L.; Ciani, G.; Proserpio, D. M. *CrystEngComm.* **2004**, *6*, 377.

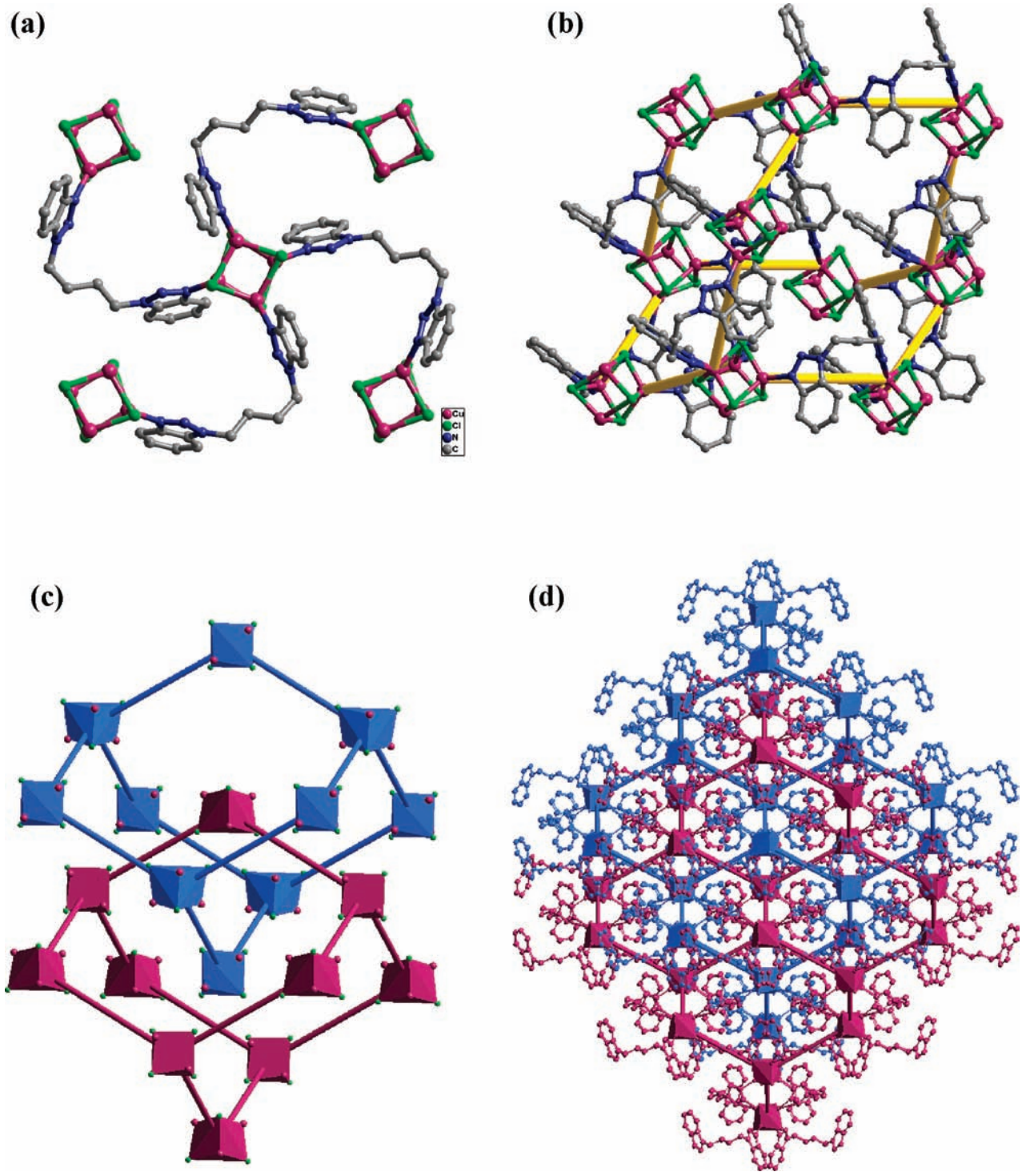

Figure 10. (a) View of the connectivity between the Cu_4Cl_4 cluster units in **10**. (b) View of a single adamantanoid cage. (c) Schematic presentation showing the two interpenetrating adamantanoid cages. (d) Two interpenetrating diamond-like 3-D frameworks in **10**.

ligands via two unoccupied N sites, and this bridging gives an unprecedented μ_4-bridging mode for the α,ω-bis(benzotriazole)alkane ligands. Accounting for two isomers of 1,3-bis(benzotriazole)propane (**L3** and **L5**) reveals that one benzotriazole group adopts a bidentate chelating coordination mode, whereas the other one is monodentate; thus, each **L3** or **L5** ligand acts as a tridentate bridging ligand in complexes **3** and **6**. Moreover, in complexes **2**, **4**, **5**, and **10**, each benzotriazole group in **L2** or **L4** adopts a monodentate coordination mode, giving a μ_2-bridging mode, as is usually observed in coordination complexes[16] with α,ω-bis(benzotriazole)alkane as the ligand. It is noticeable that there exist vacant N sites in the above-mentioned μ_2- and μ_3-coordination modes; therefore, the coordination modes of the α,ω-bis(benzotriazole)alkane ligand should be more abundant. On the other hand, the $\pi-\pi$ stacking interactions between benzotriazole rings from α,ω-bis(benzotriazole)alkane ligands (**L1**−**L5**) are observed in complexes **1**−**10** (Table 4) and clearly help to extend the supramolecular structures or stabilize the polymer architectures. In **1** and **2**, the 1-D hybrid

chains are extended into the final 2-D networks through strong aromatic $\pi-\pi$ stacking interactions, with a center-to-center distance of 3.76 and 3.69 Å, respectively. In **3**, the weak $\pi-\pi$ stacking interactions only exist in the 1-D ribbonlike structure. For **4**, **5**, and **6**, the 1-D chains or 2-D layers are finally extended into the 3-D hybrid supramolecular architectures via $\pi-\pi$ stacking interactions. Moreover, close $\pi-\pi$ contacts also occur between benzotriazole rings in the 3-D frameworks of **7**−**10**, where they stabilize these solid-state structures. Thus, it can be concluded that the $\pi-\pi$ stacking interactions between benzotriazole rings play an essential role in the formation of the framework of these Cu(I) hybrid materials.

XRPD, TGA, and Photoluminescent Properties. As shown in Figures S11−S20 in the Supporting Information, complexes **1**−**10** were characterized via X-ray powder diffraction (XRPD) at room temperature. All the XRPD patterns measured for the as-synthesized samples were in good agreement with the XRPD patterns simulated from the respective single-crystal X-ray data using the Mercury 1.4 program.

Since thermal stability is an important quality for the application of organic−inorganic hybrid materials, we also studied all complexes by means of thermal analysis in nitrogen gas at temperatures from 40 to 1000 °C. The TGA/DTA curves for complexes **1**−**10** are provided in Figures S11−S20 in the Supporting Information. The TGA curves of these complexes are similar, with all complexes remaining stable up to ca. 250 °C; above 250 °C, two weight loss steps occurred between 300 and 900 °C, except for complex **7**. The first weight loss, observed between 250 and 400 °C, resulted from the decomposition of the α,ω-bis(benzotriazole)alkane ligands. The second weight loss corresponded to the loss of halide anions or sublimation of newly formed CuX compounds. The TGA curve for **7** shows only one sharp weight loss between 292 and 929 °C, corresponding to the removal of organic molecules and cyanides (observed 70.3%, calculated 71.3%). Detailed temperatures and weight loss values for complexes **1**−**10** are given in Table S1 in the Supporting Information.

In our previous work, we explored a series of Zn/Cd-1,2,4-triazole coordination polymers or polynuclear compounds[34] with strong blue fluorescence. Owing to their ability to affect the emission wavelength and strength of the organic materials, synthesis of inorganic−organic hybrids through judicious choices of conjugated organic spacers and transition-metal centers can be an efficient method to obtain new types of electroluminescent materials, especially for d^{10} or $d^{10}-d^{10}$ systems.[35] In this paper, we reported the luminescent properties of this novel Cu(I)/X/α,ω- bis(benzotriazole)alkane organic−inorganic hybrid family in the solid state.

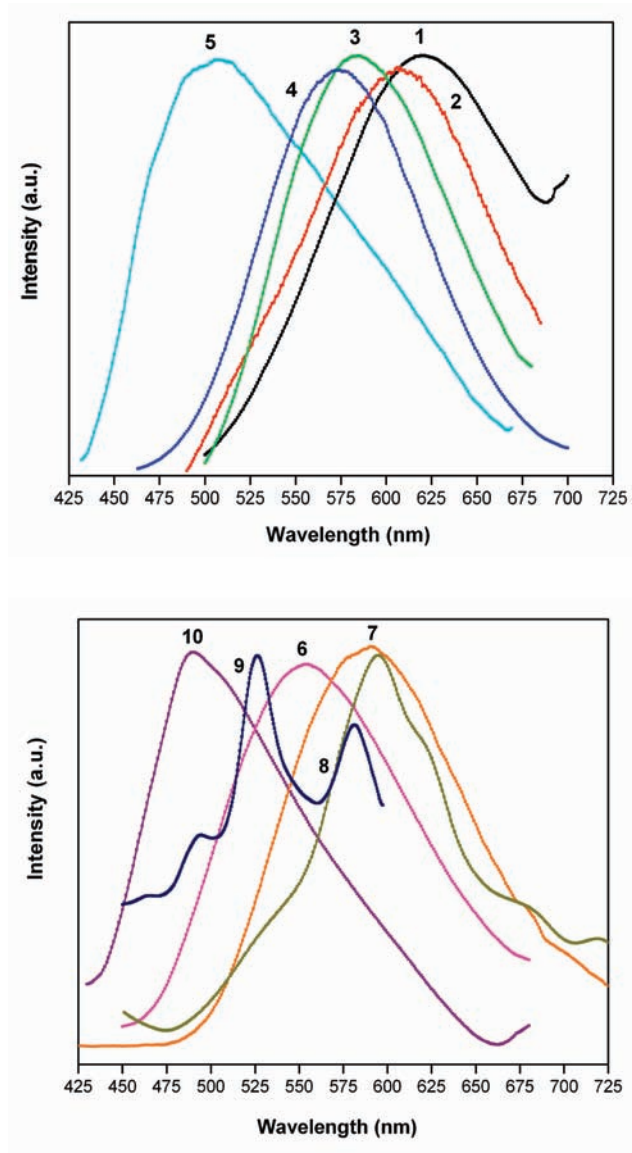

Figure 11. Emission spectra of the Cu(I) complexes in the solid state at room temperature.

Complexes **1**−**10** are stable under normal atmospheric conditions. All the complexes show strong photoluminescence upon irradiation with ultraviolet light in the solid state (Figure 11). The emission spectra of the 10 Cu(I) complexes have been recorded in the solid state at room temperature, and the spectral data are summarized in Table 5. Unfortunately, no photoluminescence measurement could be carried out in solution because the complexes cannot be dissolved in common organic solvents. Moreover, sonication was used in attempts to dissolve the complexes for solution measurements; however, these hybrid solids exhibited decomposition during sonication. Similar observations have been made by Araki et al. for other Cu(I) coordination compounds.[36]

To understand more thoroughly the nature of these emission bands, the luminescence of benzotriazole and **L1**−**L5** was also investigated. These organic molecules all show the similar emission bands at 380 ± 5 nm attributed

(34) (a) Zhai, Q. G.; Wu, X. Y.; Chen, S. M.; Lu, C. Z.; Yang, W. B. *Cryst. Growth Des.* **2006**, *6*, 2126. (b) Zhai, Q. G.; Lu, C. Z.; Chen, S. M.; Xu, X. J.; Yang, W. B. *Inorg. Chem. Commun.* **2006**, *9*, 819. (c) Zhai, Q. G.; Lu, C. Z.; Wu, X. Y.; Batten, S. R. *Cryst. Growth Des.* **2007**, *7*, 2332.

(35) (a) Seward, C.; Jia, W. L.; Wang, R. Y.; Enright, G. D.; Wang, S. N. *Angew. Chem., Int. Ed.* **2004**, *43*, 2933. (b) Yam, V. W. W.; Lo, K. K. W. *Chem. Soc. Rev.* **1999**, *28*, 323.

(36) Hiromi, A.; Kiyoshi, T.; Yoichi, S.; Shoji, I.; Noboru, K. *Inorg. Chem.* **2005**, *44*, 9667.

Table 5. Emission Data of the Cu(I) Complexes

complex	Cu−N (Å)	Cu−X (Å)	Cu···Cu (Å)	λ_{ex} (nm)	λ_{em} (nm)
1	2.037(3)−2.020(3)	2.3540(13)−2.4254(15)	3.1606(7), 3.7084(7)	355	615
2	2.040(3)−2.075(3)	2.4578(6)−2.5355(6)	2.9138(6)	355	610
3	1.794(4)−2.307(5)	1.9955(15)−2.681(2)	3.4548(15), 4.0289(14)	354	584
4	2.024(11)−2.026(12)	2.628(2)−2.851(2)	2.6345(51)−2.7279(48) Å	356	568
5	2.006(3)	2.5074(7)−2.5658(7)	2.7681(8)−2.8314(8)	342	507
6	2.008(5)−2.032	2.4192(11)−2.6561(12)	2.8942(14)−3.2687(14)	355	556
7	2.099(5)−2.173(5)	1.917(10)−1.976(8) (CN)	5.0068(19), 5.0263(18)	340	590
8	1.956(4)−2.010(4)	2.2022(16)−2.6313(17)	2.9817(5)−4.1747(10)	377	594
9	1.946(19)−2.055(15)	2.320(17)−2.69(4)	2.6083(17)−4.4847(38)	389	490, 525, 581
10	1.966(7)−1.971(7)	2.354(3)−2.523(3)	2.9009(23)−3.0740(22)	355	489

to the intraligand $\pi-\pi^*$ transitions, and no fluorescent bands were observed in the range of 400−800 nm. Several reports show that the emission energies of copper(I)−halide complexes are strongly affected by the N-heteroaromatic ligand, and several possible lowest excited states have been suggested to date.[37] These include metal-to-ligand charge transfer (MLCT), single metal-centered transitions (MC), halide-to-ligand charge transfer (XLCT), ligand-centered transitions (LC), and cluster-centered transitions (CC). Henary et al. reported that the emission of $[Cu_2(\mu\text{-}Cl)_2(PPh_3)_2(pyz)]$ should be attributed to MLCT, on the basis of resonance Raman spectroscopy.[38] Ford et al. reported the emission of a series of py complexes $[(Cu_2(\mu\text{-}X)_2(PPh_3)_2)(py)_2]$ (X = I, Br, Cl) and pointed out the possibility of the XLCT excited state.[39a] They also reported that the emission of $[Cu_2(\mu\text{-}I)_2(py)_4]$ is mainly attributed to both CC transition and XLCT.[39b]

Consistent with these previously reported complexes of cuprous halides and heterocyclic ligands, we tentatively assigned the emission of these Cu(I) complexes as being a combination of a metal-centered state modified by the Cu···Cu interaction and a MLCT or XLCT state, due to their broad and structureless emission spectra, as benzotriazole ligands do not show photoluminescence in the range of 400−800 nm. The emission peaks for **1** and **2** are similar, with only a 5 nm difference in the red range, which is in agreement with their similar Cu_2X_2 inorganic subunits and similar extended 1-D chain hybrid architectures. For complexes **4**, **5**, and **10**, which have similar cubane clusters only with a different X, the large red shift of the emission maximum from 489 (**10**, CuCl type) to 507 (**5**, CuBr type) and 568 nm (**4**, CuI type) can be ascribed to the electron-donating ability of X because the energies of the HOMO or LUMO of the systems would certainly depend on the extent of mixing due to the XLCT.[36] However, two sharp emission bands at 525 and 581 nm along with a weak shoulder bond at 490 nm of **9** could be related to the short Cu−Cu contact distances of 2.6083 Å; the high-energy emission originates from a triplet metal-centered 3d → (4s, 4p) excited state modified by a Cu···Cu interaction.[40] Those phenomena are distinctly different from the isomorphic complex **8**.

In the case of complex **7**, the CN^- anions maybe play a similar role as halogen in other hybrid compounds. However, XLCT, CC, and LC transitions may be ruled out since metal−metal bonding is negligible and cyanide has a fairly large band gap. Pike et al.[41] reported that the emission band at 392 nm for CuCN should be ascribed to invoke MC transitions of the type 3d → (4p, 4s). They also reported that the peak broadening and red shift for $(CuCN)_{20}(pip)_7$ (pip = piperazine), compared to that of CuCN, were due to the incorporation of pip ligands and a heterogeneous array of copper(I) centers. Taking the position and broad shape into account, the emission of **7** may also be reasonable and consistent with the MC transitions influenced by the existence of benzotriazole ligands.

Conclusion

Five flexible bis(benzotriazole)alkane ligands were prepared by the reaction of benzotriazole with dibromoalkane and were exploited for the first time to prepare 10 hybrid materials based on copper(I) halides or pseudohalides using hydro(solvo)thermal methods. All 10 compounds incorporated charge-balancing anions, in addition to the flexible benzotriazolate group, to provide hybrid materials of the general type Cu(I)/X/α,ω-bis(benzotriazole)alkane (X = Cl, Br, I, or CN). The ability of bis(benzotriazole)alkane ligands to bridge two, three, or four metal centers contributed to the remarkable structural diversity of the ternary Cu(I)/X/α,ω-bis(benzotriazole)alkane materials. The synergism of the potentially polydentate bridging of the flexible benzotriazolate and the effectiveness of the halide or pseudohalide anions in adopting various bridging modes provided complex connectivity patterns and the synthesis of materials with higher dimensions. Thus, all the complexes present extended architectures with increasing dimensionality from 1-D (**1**−**4**) to 2-D (**5** and **6**) to 3-D (**7**−**10**). The structural chemistry of metal halides or pseudohalides is complex, with the identities of both the metal and the anion (X^-) acting as significant structural determinants. This observation is reinforced by the range of inorganic component substructures revealed by the materials in our study: $\{Cu_2X_2\}$ binuclear clusters (**1** and **2**), $\{Cu_4X_4\}$ cubane clusters (**4**, **5**, and **10**), $\{CuX\}_n$ single chains (**3** and **7**), $\{Cu_3X_3\}_n$ ladderlike chains (**6**), and unprecedented $\{Cu_8X_8\}_n$ ribbons (**8** and **9**). The structural and compositional complexity of this hybrid system can be further enhanced by the synthesis conditions we exploited

(37) Kutal, C. *Coord. Chem. Rev.* **1990**, *99*, 213.
(38) Henary, M.; Wootton, J. L.; Khan, S. I.; Zink, J. I. *Inorg. Chem.* **1997**, *36*, 796.
(39) (a) Ford, P. C.; Cariati, E.; Bourasssa, J. *Chem. Rev.* **1999**, *99*, 3625. (b) Vitale, M.; Ryu, C. K.; Palke, W. E.; Ford, P. C. *Inorg. Chem.* **1994**, *33*, 561.
(40) Fu, W. F.; Gan, X.; Che, C. M.; Cao, Q. Y.; Zhou, Z. Y.; Zhu, N. N. Y. *Chem.—Eur. J.* **2004**, *10*, 2228.
(41) Pike, R. D.; deKrafft, K. E.; Ley, A. N.; Tronic, T. A. *Chem. Commun.* **2007**, 3732.

to isolate these complexes. The hydrothermal domain is complicated, with variables such as time, temperature, the stoichiometries of the reactants, pH, nucleation and growth rates, and the starting materials requiring careful study and control during the synthesis reaction. However, what is evident from this study and others in the emerging field of metal−polyazaheterocycle chemistry is the certainty that huge numbers of materials with unusual, unprecedented, and formerly inconceivable structures remain to be discovered. Furthermore, their strong photoluminescent properties indicate that these condensed hybrid materials may be excellent candidates for potential photoactive materials since they are thermally stable and insoluble in common polar and nonpolar solvents. On the basis of this work, further syntheses and studies of the structures and properties of hybrid systems consisting of other flexible benzotriazole ligands and metal halide or pseudohalide substructures are underway in our laboratory.

Acknowledgment. This work was supported by the Natural Science Foundation of China (Grant Nos. 20801033 and 20871079), the National High Technology Research and Development Program of China (2007AA03Z248), and the Youth Foundation of Shaanxi Normal University.

Supporting Information Available: X-ray crystallographic files, additional plots of the structures, XRPD, and thermogravimetric analysis data for the complexes. This material is available free of charge via the Internet at http://pubs.acs.org.

IC801574K